State of Delaware
DELAWARE GEOLOGICAL SURVEY
David R. Wunsch, Director

OPEN FILE REPORT No. 54

BEDROCK GEOLOGIC MAP OF THE DELAWARE PIEDMONT

By:

William S. Schenck

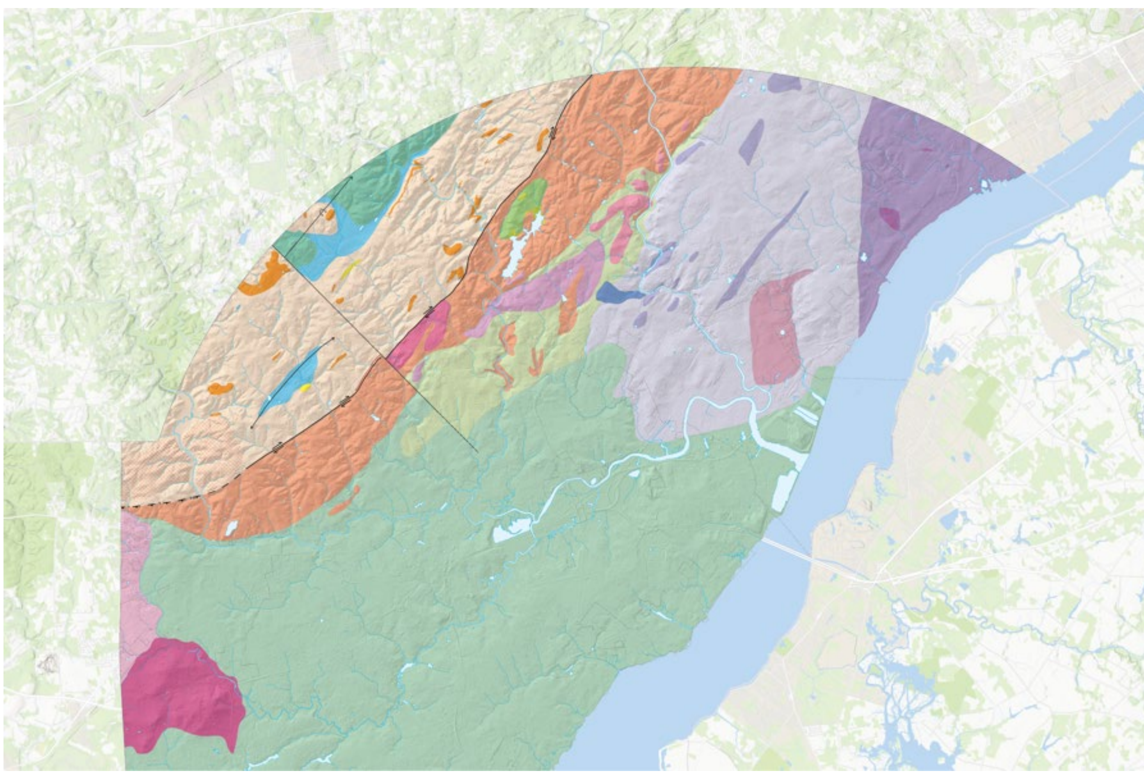

University of Delaware
Newark, Delaware
2021

TABLE OF CONTENTS

FIGURES

PLATES

INTRODUCTION

The Piedmont rock units in Delaware, and bedrock geologic map of Schenck et al. (2000) are revised in this report based on new rock geochemistry, geochronometric data, petrography, and recent detailed mapping. Major revisions include:

- revising the extent of the Christianstead Gneiss and Windy Hills Gneiss
- abandoning the Wissahickon Formation as originally mapped in Delaware by Bascom (1902, 1905) and Bascom et al. (1909, 1920, and 1932) and replacing it with the Mt. Cuba Gneiss, a lithodeme of the West Grove Metamorphic Suite (Bosbyshell et al., 2012, 2013, 2014, 2015), and reserving the Wissahickon Schist/Formation for the metasediments on the east side of the Wilmington Complex magmatic arc and referring to them herein as Wissahickon Formation (restricted sense)
- extending the Rosemont Shear Zone from Pennsylvania southwest through Delaware to Maryland separating the Mt. Cuba Gneiss and the Wilmington Complex
- formally naming and describing two new units in the Wilmington Complex - the Greenville Gabbro and the Thompsons Bridge Gneiss.

The previous model for the geologic history of the Delaware Piedmont (Plank et al., 2000) was based on eastward-dipping subduction and closure of a forearc basin thereby emplacing and thrusting magmatic arc crust over forearc basin sediments, nearshore deposits, and continental crust during the Taconic orogeny. In this model, the boninitic affinity of amphibolite in the Rockford Park Gneiss confirmed the early subduction of young, hot lithosphere. Subsequent thrusting, which happened as the arc was obducted onto the ancient continent, was borne out by the presence of the Mill Creek, Avondale, and West Chester nappes.

Based on recent studies and detrital zircon analyses, Bosbyshell et al. (2015) proposed that the Wilmington Complex with its associated metasediments may have been part of the Taconic Arc in New England and translated by strike-slip deformation to its present location. In the Central Appalachian Piedmont, middle to late Paleozoic transpressive deformation with significant strike-slip is associated with the Pleasant Grove – Huntingdon Valley Shear Zone and the Rosemont Shear Zone with as much as 150 km of dextral displacement (Valentino et al. 1994, 1995). Bosbyshell et al. (2015) also proposed extending the Rosemont Shear Zone southwest through Delaware to Maryland separating the West Grove Metamorphic Suite and the Wilmington Complex. The geology presented herein follows this model of emplacement of the Wilmington Complex magmatic arc and associated metasediments through transpression along the dextral Pleasant Grove – Huntingdon Valley Shear Zone and the Rosemont Shear Zone. This final emplacement may have been the result of younger movement in the Pleasant Grove – Huntingdon Valley Shear Zone, which was active into the Pennsylvanian-Permian Alleghenian orogeny (Valentino and Gates, 2001; Blackmer et al., 2007).

Plate 1 of this report is a bedrock geologic map with soil, regolith, and surficial deposits of Quaternary age removed. Where data are available (Table 1, Plate 1), Delaware's Piedmont rock units are modified and extended beneath the Coastal Plain as far south as Iron Hill.

For a digital representation of the map, the geologic lines and polygons are available for download on the Delaware Geological Survey (DGS) website. The geologic polygons are also available to view on a mobile device or personal computer through an online web mapping application.

ACKNOWLEDGEMENTS

I would like to gratefully acknowledge and thank the "Piedmont Group" of geologists I have worked with since the early 1990s, without whose help this revision would not be possible. These geologists include Gale Blackmer, Pennsylvania Geological Survey; Howell (Hal) Bosbyshell and LeeAnn Srogi, West Chester University; Margaret (Peg) Plank, formerly DGS; and Heather Quinn and William (Will) Junkin, Maryland Geological Survey. I acknowledge and thank Lillian Wang, DGS, for her artistic help with figures and cartographic/GIS creation of the map and online mapping application, and Paul (Steve) McCreary and others at the DGS, without whose help I could not have obtained subsurface samples to extend the Piedmont rock units beneath the Delaware Coastal Plain. I also dedicate this revised map to Peg Plank and name a new lithodemic rock unit within the Wilmington Complex, the Thompsons Bridge Gneiss, in honor of Dr. Allan M. Thompson, associate professor emeritus, University of Delaware, Department of Earth Sciences.

CHANGING THE EXTENTS OF THE CHRISTIANSTEAD GNEISS AND WINDY HILLS GNEISS

Boreholes drilled to basement through the Delaware Coastal Plain south of the Fall Line to Iron Hill have enabled a petrographic analysis of new basement core and outcrop samples (Table 1, Plate 1). The new analyses resulted in a reinterpretation of the basement rock in the area of Iron Hill near Newark, Delaware. Just north of Iron Hill and east of the Christiana River, basement is mapped as the Windy Hills Gneiss, rather than as the Christianstead Gneiss previously mapped by Schenck et al. (2000). The Christianstead Gneiss now extends from Iron Hill to the northwest from the Christina River to the Maryland State Line. Petrographic data for many of these samples and all other DGS thin section data are distributed through the DGS Petrographic Data Viewer (Open File Report No. 55).

The contact between the Windy Hills Gneiss and the Brandywine Blue Gneiss (Plate 1) is modified from Schenck et al. (2000) based on the geochemistry of a mafic layer exposed at Canby Park, located in Wilmington, Delaware (T. A. Plank, written communication, May 2019). This outcrop, shown as CANBY in Figure 1, is outcrop Cc15-b (Table 1, Plate 1). Schenck et al. (2000) assumed Canby Park was covered by Coastal Plain sediments; however, further mapping in 2014 revealed bedrock exposed in Little Mill Creek, which runs through the park. The rocks are interlayered mafic and felsic gneisses comparable to the Windy Hills Gneiss and Rockford Park Gneiss. Plank's geochemical analysis of the mafic layer at Canby Park shows the amphibolite is a depleted arc tholeiite basalt similar to the mafic layers within the Windy Hills Gneiss and are not boninitic like the mafic layers in the Rockford Park Gneiss (Fig. 1, and Appendix 1). Samples WINDY (Group IV - Plank et al. 2001) and ROCKFORD (Group I - Plank et al. 2001) shown in Figure 1 are outcrops Cb42-c and Bd41-b, respectively (Table 1, Plate 1).

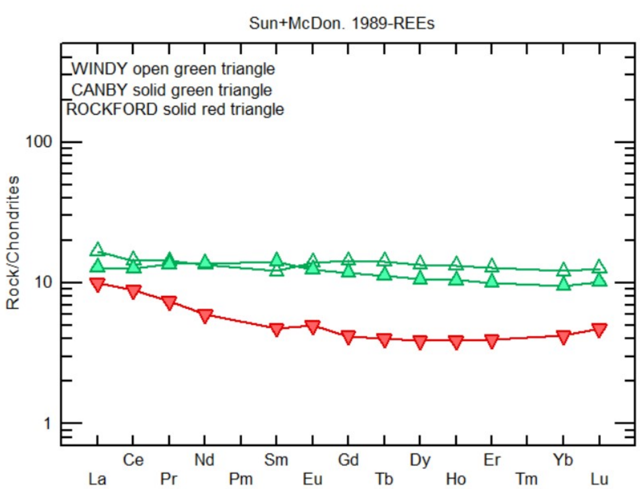

Figure 1. Rare Earth Element (REE) patterns for samples WINDY, CANBY, and ROCKFORD.

SEPARATING THE WISSAHICKONS

Bascom (1902) named a belt of mica-schist and gneiss extending from northeast of Philadelphia southwest to Maryland the Wissahickon Schist after outcrops exposed along Wissahickon Creek in Philadelphia, Pennsylvania. Mathews (1905) extended the Wissahickon into the area of Baltimore, Maryland, and further into northern Virginia by referring to those schists and gneisses as the Wissahickon Formation. Bascom (1905) expanded the extent of the Wissahickon Formation to include the mica schists flanking Mine Ridge and the Honeybrook Upland in southeastern Pennsylvania. Thus, by 1905, nearly all the psammitic and pelitic gneisses, schists, and phyllites in the central Appalachian Piedmont were mapped as the Wissahickon Formation. Since that time, the Wissahickon Formation has been extensively studied and the stratigraphic nomenclature continuously revised. Pavlides (1974) removed the Wissahickon nomenclature from the Virginia geologic map. Crowley (1976) created the Wissahickon Group and renamed the Wissahickon Formation in the Maryland Piedmont near Baltimore as the Lock Raven and Oella Formations. For a complete summary of the history of the Wissahickon Formation in the central Piedmont refer to Schenck (1997).

Faill (1997) suggested informal terms of "Glenarm Wissahickon" for the mica schists and gneisses associated with the Cockeysville Marble and Setters Quartzite of the Glenarm Group west of the Wilmington Complex, and "Philadelphia Wissahickon" for the type section Wissahickon Formation (restricted sense) east of the Wilmington Complex near Philadelphia. Schenck et al. (2000), recognized that the metasediments along the western side of the Wilmington Complex were interlayered with metavolcanic units and informally called this unit "Arc Wissahickon" in order to separate it from the "Glenarm Wissahickon" and the Wissahickon Formation (restricted sense). The data to support this separation were sparse; therefore, Schenck et al. (2000) published these metasediments as Wissahickon Formation and the metasediments comingled with the Wilmington Complex arc as Wissahickon(?).

Blackmer (2005) further restricted the Glenarm Wissahickon of Faill (1997) to the pelitic and psammitic gneisses and schists north of the Avondale Anticline in Pennsylvania and mapped the rest of the metasediments from the Avondale Anticline southeast to the Wilmington Complex informally as "Mt. Cuba Wissahickon." Based on detrital zircon analysis, Bosbyshell et al. (2013, 2014,

2015) proposed and defined a new lithodemic suite called the West Grove Metamorphic Suite. The Suite includes lithodemes of Doe Run Schist, Laurels Schist, Mt. Cuba Gneiss, Kennett Square Amphibolite, and White Clay Creek Amphibolite. The lithodemes of Doe Run Schist, Laurels Schist, and Mt. Cuba Gneiss in the West Grove Metamorphic Suite replace the Glenarm Wissahickon of Faill (1997), the Mt. Cuba Wissahickon of Blackmer (2005), and finally divide what was originally mapped as Wissahickon in the central Piedmont into the West Grove Metamorphic Suite west of the Rosemont Shear Zone and the Wissahickon Formation (restricted sense) east of the Rosemont Shear Zone.

Additional detrital zircon analyses of three samples (Bc54-g, Cb42-d, and Bd21-j) from the strip of pelitic and psammitic gneisses on the western side of the Wilmington Complex in Delaware ("Arc Wissahickon") suggest they are correlative with the Wissahickon Formation (restricted sense) and not with the Mt. Cuba Gneiss (Fig. 2, Plate1, Table1, Appendix 3; R. Mathur and H. Bosbyshell, written communication December 2020). Bounded by the Rosemont Shear Zone on the west and interlayered with the Faulkland and Windy Hills metavolcanic units of the Wilmington Complex on the east, these gneisses are mapped herein as a new lithodeme of the Wilmington Complex called Thompsons Bridge Gneiss. The Thompsons Bridge Gneiss is Ordovician in age, and it is correlative with, but not connected to, the Wissahickon Formation (restricted sense). This also suggests the Wissahickon Formation units (restricted sense) on the east side of the arc could be included as additional lithodemes within the Wilmington Complex.

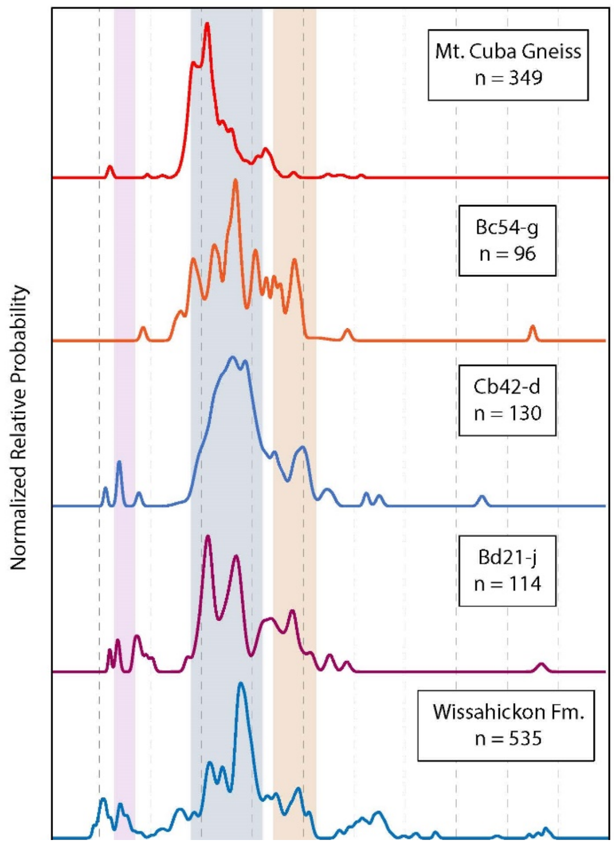

Figure 2. Detrital zircon ages for three samples of Thompsons Bridge Gneiss with detrital zircon ages for Mt. Cuba Gneiss and Wissahickon Formation (restricted sense) for comparison. Purple shading – Gondwana, Laurentia; gray shading – Grenville, and Laurentia; tan shading – Granite-Rhyolite province.

Plank et al. (2000) suggested that the Wilmington Complex arc continued into Cecil County, Maryland, and that the James Run units mapped by Higgins and Conant (1986) and Higgins (1990) were most likely units within the Wilmington Complex. A recent crystallization zircon age analysis on a sample from Big Elk Creek at Fair Hill, Maryland, and type section for the Big Elk Member of the James Run Formation (not shown on Plate 1) has yielded an igneous crystallization age of 463±5 Ma for this James Run unit (R. Mather, written communication November 2019, Appendix 2). In contrast, the igneous crystallization age of the nearby Windy Hills Gneiss of the Wilmington Complex is significantly older, 481±4 Ma (Aleinikoff et al., 2006). This age difference indicates that the younger James Run units could lie above the Windy Hills Gneiss or be partially juxtaposed by an oblique thrust of the Rosemont Shear Zone as it turns slightly to the southwest and west entering Maryland. Recent studies suggest the Rosemont Shear Zone, or a splay of the shear zone may turn southwest crossing into Maryland (J.W. Horton Jr., written communication, April 2020). Further study is needed to fully understand the complexities in this area.

DEFINITION OF NEW MAP UNITS

With the exception of the Mt. Cuba Gneiss, Thompsons Bridge Gneiss, and the Greenville Gabbro, which are described herein, Plate 1 shows the same rock units of Schenck et al. (2000), which are described in detail in Plank et al. (2000).

Mt. Cuba Gneiss

(herein adopted for Delaware Piedmont rocks previously mapped as Wissahickon)

Definition. The Wissahickon Formation mapped by Schenck et al. (2000) is renamed the Mt .Cuba Gneiss. The name Wissahickon is abandoned for any rocks originally mapped in Delaware as Wissahickon Schist or Formation by Bascom (1902, 1905), Bascom et al. (1909, 1920, and 1932), and Schenck et al. (2000). The name Wissahickon Schist or Formation (restricted sense) is reserved for metasediments east of the Wilmington Complex in southeastern Pennsylvania (Bosbyshell et al., 2012, 2013, 2014, 2015, this report).

The Mt. Cuba Gneiss is a lithodeme within the West Grove Metamorphic Suite consisting of psammitic and pelitic gneisses with amphibolite (Bosbyshell et al., 2013, 2015). It is named for rocks at Mt. Cuba, Delaware. The Mt. Cuba Gneiss is mapped within the Oxford, West Grove, Kennett Square, Wilmington North, Newark West, Newark East, and Wilmington South 7.5-minute quadrangles.

Historical Background. Originally mapped as Wissahickon Formation by Schenck et al. (2000), detrital zircon age analysis of these pelitic and psammitic gneisses with amphibolite requires the separation from the Wissahickon Formation (restricted sense) mapped by Florence Bascom and others from the type locality in Philadelphia (Bosbyshell et al., 2012, 2013, 2014). Bosbyshell et al. (2013, 2014, 2015) proposed and defined the West Grove Metamorphic Suite that includes lithodemes of Doe Run Schist, Laurels Schist, Mt. Cuba Gneiss, Kennett Square Amphibolite and White Clay Creek Amphibolite. The names Mt. Cuba Gneiss and the White Clay Creek Amphibolite within it, are adopted for the pelitic and psammitic gneisses with amphibolite west of the Rosemont Shear Zone in Delaware and are the only units of the West Grove Metamorphic Suite shown on Plate 1.

Boundaries. The Mt. Cuba Gneiss extends southeast from the Avondale Anticline in Pennsylvania (3.5 miles northwest of the Delaware state boundary) to the Rosemont Shear Zone and the contact with the Wilmington Complex Thompsons Bridge Gneiss (*herein named*) and south to include the units mapped as pelitic schist, pelitic schist with amphibolite, and pelitic gneiss in northeastern Cecil County, Maryland (Higgins and Conant, 1986; Higgins, 1990; Blackmer, 2005).

Lithology. In Delaware, the Mt. Cuba Gneiss consists of pelitic and psammitic gneisses with amphibolite. Granitic pegmatite as layers and pods is ubiquitous throughout the unit. Pelitic and psammitic lithologies are mainly quartz-plagioclase-biotite gneiss with or without garnet and sillimanite. The rocks have been metamorphosed to amphibolite facies, display partial melting, and in places are isoclinally folded. Metamorphism increases from west to east within the map area (Plate 1). The lowest grade assemblage of quartz, biotite, plagioclase, orthoclase, sillimanite, muscovite, and ilmenite ± garnet occurs in the southwestern portion of the Mt. Cuba Gneiss. Toward the northeast, muscovite gradually disappears from the assemblages and is missing from the rocks east of Red Clay Creek.

Layers of amphibolite in the Mt. Cuba Gneiss include two geochemical types, the Kennett Square Amphibolite and the White Clay Creek Amphibolite (Smith, 2004; Smith and Barnes, 2004). The Kennett Square Amphibolite has ocean floor geochemistry and is found primarily in Pennsylvania northwest and north of the Hockessin-Yorklyn Anticline and the Delaware state boundary. The White Clay Creek Amphibolite with continental initial rift geochemistry is found primarily south and southeast of the Hockessin-Yorklyn Anticline to the contact with the Wilmington Complex in Delaware (Blackmer, 2005).

The Mt. Cuba Gneiss is in depositional contact with the Glenarm Group containing the Setters Formation and the Cockeysville Marble (Blackmer 2005, Bosbyshell et al., 2014). The Glenarm Group is exposed through antiformal uplifts but may also be tectonically emplaced inliers of marble and near-shore sediments originally deposited along the Laurentian coast (Blackmer, 2005).

Primary sedimentary structures have been obliterated by deformation, metamorphic differentiation, and partial melting; however, quartz-rich psammitic layers alternate with biotite-sillimanite rich layers on a scale of 3 to 4 inches and may represent deposition by submarine turbidity currents along the rift-drift Laurentian margin.

Age. Electron probe U-Th-total Pb age microanalysis (EPMA) of monazite within the Mt. Cuba Gneiss indicates a Silurian age of metamorphism (Blackmer, 2005, Bosbyshell et al., 2016). Recent detrital zircon studies

(Bosbyshell et al., 2012, 2013, 2014) show this body of rock is dominated by 960-1500 Ma peaks with the youngest zircon ages at 530-560 Ma suggesting these metasediments can be no older than Cambrian and are consistent with early Paleozoic Laurentian margin sediments.

Type Section. The type section for the Mt. Cuba Gneiss is outcrop Bc32-am, an extensive outcrop located along the entrance drive at Mt. Cuba Center at Mt. Cuba, Delaware. (Fig. 3, Table 1, Plate 1).

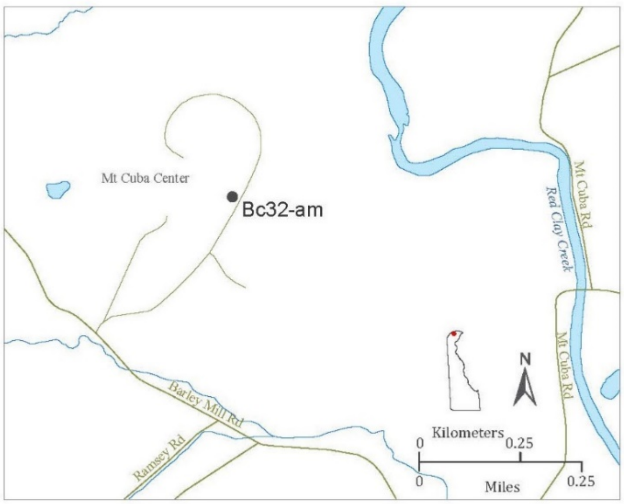

DGSID	Northing UTM-18 (m)	Easting UTM-18 (m)	Lithology
Bc32-am	*4404401.683*	*444559.647*	*Pelitic and psammitic gneisses with amphibolite*

Figure 3. Type section outcrop of Mt. Cuba Gneiss, Mt. Cuba, Delaware.

Thompsons Bridge Gneiss

(herein named)

Definition. The Thompsons Bridge Gneiss (*herein named*) is a new lithodeme within the Wilmington Complex. The lithodeme consists of pelitic and psammitic gneisses along the western side of the Wilmington Complex magmatic arc, which was previously mapped as the Wissahickon Formation and metasediments interlayered with metavolcanic units mapped as Wissahickon(?) by Schenck et al. (2000). The name is the geographic locality of the type section in Delaware and also pays homage to Allan M. Thompson, Ph. D, one of the first geologists to map the rocks of the Delaware Piedmont at 1:24,000 scale (Woodruff and Thompson, 1972, 1975). The Thompsons Bridge Gneiss is located within the Newark West, Newark East, Kennett Square, and Wilmington North 7.5-minute quadrangles.

Historical Background. These pelitic and psammitic gneisses were originally mapped as Wissahickon Formation and Wissahickon(?) by Schenck et al. (2000). Recent detrital zircon analysis (Ryan Mathur and Howell Bosbyshell, this report) requires this lithodeme of pelitic and psammitic gneisses to be separated from the Mt. Cuba Gneiss. This report and map include these gneisses as a new lithodeme within the Wilmington Complex and correlative with the Wissahickon Formation (restricted sense) because they are not physically connected to the Wissahickon metasediments on the eastern side of the Wilmington Complex arc.

Boundaries. The Thompsons Bridge Gneiss is separated from the Mt. Cuba Gneiss by the Rosemont Shear Zone and extends the length of the Wilmington Complex from Pennsylvania southwest to Cecil County, Maryland.

Lithology. The major lithologies in the Thompsons Bridge Gneiss are pelitic and psammitic gneisses and quartzites, with or without abundant sillimanite and garnet. Flaser and ribbon textures are common near and along the Rosemont Shear Zone and throughout the unit within the Delaware Piedmont. The unit has been metamorphosed to amphibolite and upper amphibolite facies and, in places, isoclinally folded. Metamorphic differentiation in the pelitic and psammitic rocks has separated quartzofeldspathic layers from layers rich in biotite, sillimanite, and garnet. Garnets from 1 mm to 1.5 cm occur within in the psammitic and pelitic lithologies and, where associated with abundant biotite, sillimanite, and locally cordierite, spinel, and corundum, are restite from in-situ partial melting. Sillimanite is concentrated in the pelitic lithologies as a matrix mineral, in flattened nodules that vary from 5 mm to 5 cm in diameter, in veins approximately 1 mm- to 1-cm thick, and in large fibrous clumps from 0.5 to 1 meter in diameter. Brandywine Springs Park, located within the Faulkland Gneiss, is renowned for the large boulders of sillimanite that can be found along the banks of the Red Clay Creek and its tributaries. Sillimanite boulders have not been observed in outcrop. It is assumed they formed in the aluminous pelitic gneisses at or near contacts with metavolcanic and metaigneous units that occur throughout Brandywine Springs Park. An ultramafic lens composed of cumulus layers of serpentinized peridotite, metapyroxenite, and metagabbro occurs near Hoopes Reservoir.

Age. The age of the Thompsons Bridge Gneiss is Ordovician as it shares an interlayered contact with the Faulkland and Windy Hills metavolcanic units of the Wilmington Complex. The Faulkland Gneiss and Windy Hills Gneiss have igneous ages of crystallization of 482±4 and 481±4 Ma, respectively (Aleinikoff et al., 2006). Detrital zircon analysis (Ryan Mathur and Howell Bosbyshell, this report) shows the Thompsons Bridge Gneiss to be correlative with, but not connected to, the Ordovician-Silurian Wissahickon Formation (restricted sense) in Pennsylvania near Philadelphia.

Type Section. The type section for the Thompsons Bridge Gneiss consists of large exposures of sheared psammitic and pelitic gneiss at Thompsons Bridge in Brandywine Creek State Park, Delaware, outcrop Bd21-j (Fig. 4, Table 1, Plate 1). An additional reference section is outcrop Cb42-d along Middle Run near Newark, Delaware (Fig. 4a, Table 1, Plate 1).

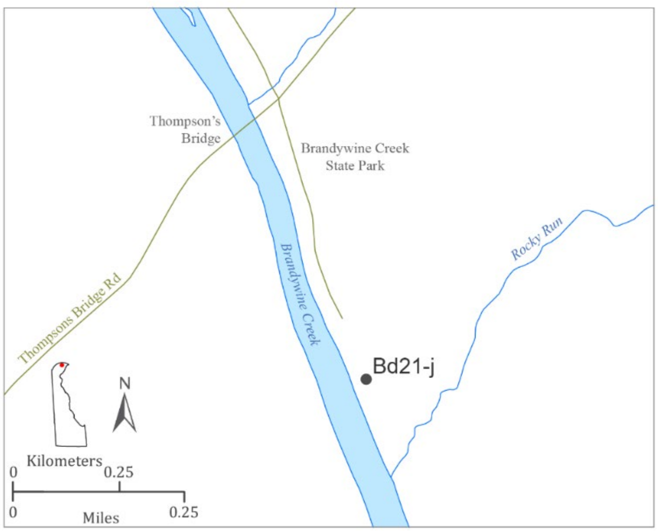

DGSID	Northing UTM-18 (m)	Easting UTM-18 (m)	Lithology
Bd21-j	4407145.8	451454.2	*Pelitic and psammitic gneisses*

Figure 4. Type section outcrop of Thompsons Bridge Gneiss, Thompsons Bridge, Delaware.

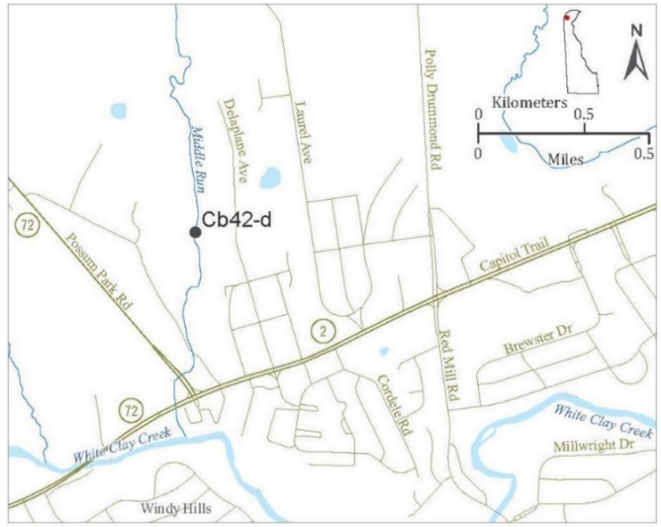

DGSID	Northing UTM-18 (m)	Easting UTM-18 (m)	Lithology
Cb42-d	4394704.2	438314.6	*Pelitic and psammitic gneisses*

Figure 4a. Reference section outcrop of Thompsons Bridge Gneiss, Middle Run, Newark, Delaware.

Greenville Gabbro
(herein named)

Definition. The Greenville Gabbro (*herein named*) is an undeformed gabbroic pluton near Greenville, Delaware. The best exposures of this gabbro occur in outcrop Bd41-a at the Henry Clay Bridge over the Brandywine Creek, and boulders (outcrops Bc45-f, g, h, i, j, k, l, n) in a meadow along Brecks Lane, Wilmington, Delaware (Table 1, Plate 1). Additional samples from core drilling (DGS core collection Bc45-11, 14, 15) also offer excellent examples of this unit. The Greenville Gabbro is located within the Wilmington North quadrangle.

Historical Background. The Greenville Gabbro was discovered in 2013 while conducting reconnaissance field work for Piedmont drill sites. Boulders of coarse-grained gabbro were found in an abandoned railroad underpass beneath Route 52 near Greenville, Delaware, and in an adjacent meadow along Brecks Lane. Schenck et al. (2000) had known of the existence of one coarse-grained gabbro boulder at the water tower in Rockford Park, Wilmington. This was confusing at the time because the nearest gabbro was the Bringhurst Gabbro, 3.5 miles east. The discovery of gabbro at the Henry Clay Bridge and around Brecks Lane only 0.2 miles away from Rockford

Park now explains how a gabbro boulder could be at the water tower. Six core holes were drilled in 2014 to determine the extent of the gabbro.

Boundaries. The Greenville Gabbro intruded and stitched the Brandywine Blue Gneiss and Faulkland Gneiss in the area just south and east of Greenville, Delaware. The unit extends from Route 141 to the Brandywine Creek near the DuPont Experimental Station below Rockford Park, Wilmington. Coarse-grained boulders in Brecks Lane meadow mark the interior of the pluton while finer grained gabbronorite, or lack of gabbro in drill holes helped map the edges of the pluton. Due to the development in the area, its contacts with the Faulkland Gneiss and Brandywine Blue Gneiss are not exposed.

Lithology. The Greenville Gabbro is black, fine- to coarse-grained gabbronorite with subophitic textures and little to no metamorphism. The primary minerals are clinopyroxene, plagioclase, hornblende, and minor orthopyroxene.

Age. Like the other igneous plutonic rocks in the Delaware Piedmont - Arden Plutonic Supersuite, Bringhurst Gabbro, Iron Hill Gabbro - this small body of gabbro is presumed to be Silurian. These Silurian plutons high-heat flow and associated mantle-derived magmatism resulted in granulite-grade metamorphism, with highest temperatures along pluton margins within the Wilmington Complex.

Type Section. The type section for the Greenville Gabbro is a large exposure near the bridge across the Brandywine Creek, outcrop Bd41-a, as well as boulders exposed in a meadow south of Brecks Lane (Fig. 5, Table 1, Plate 1).

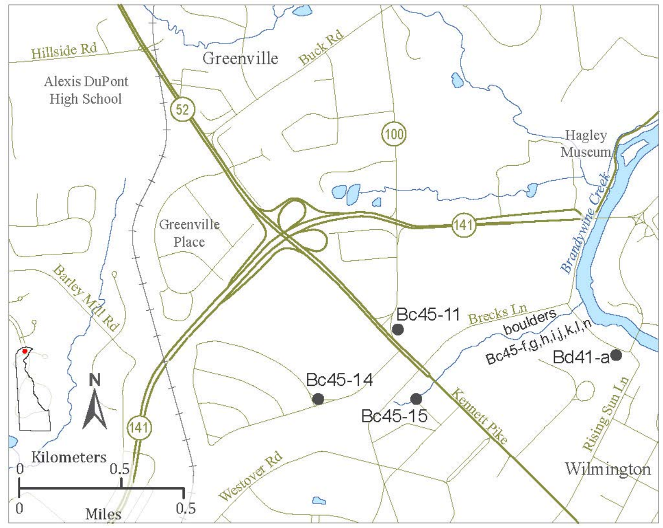

DGSID	*Northing UTM-18 (m)*	*Easting UTM-18 (m)*	*Lithology*
Bd41-a	4402262.6	450499.3	*Gabbronorite*

Figure 5. Type section outcrop of Greenville Gabbro, Greenville, Delaware.

REFERENCES CITED

Aleinikoff, J.L., Schenck, W.S., Plank, M.O., Srogi, L.A., Fanning, C.M., Kamo, S.L., and Bosbyshell, H., 2006, Deciphering igneous and metamorphic events in high-grade rocks of the Wilmington Complex, Delaware: Morphology, cathodoluminescence and backscattered electron zoning, and SHRIMP U-Pb geochronology of zircon and monazite: Geological Society of America Bulletin, v. 118, p. 39–64.

Bascom, F., 1902, The geology of the crystalline rocks of Cecil County: Maryland Geological Survey, Cecil County Report, p. 83-148.

___, 1905, Piedmont district of Pennsylvania: Geological Society of America Bulletin, v. 16, p. 289-328.

Bascom, F., Clark, W.B., Darton, N.H., Kummel, H.B., Salisbury, R.D., Miller, B.L., and Knapp, G.N., 1909, Description of the Philadelphia district-Philadelphia folio: U. S. Geological Survey Geological Atlas of the United States, Folio 162, 24 p. with maps, scale 1:62,500.

Bascom, F., and Miller, B.L., 1920, Description of the Elkton and Wilmington quadrangles, Elkton-Wilmington Folio: U. S. Geological Survey, Geologic Atlas of the United States, Folio 211, 22 p. with maps, scale 1:62,500.

Bascom, F., and Stose, G.W., 1932, Description of the Coatesville and West Chester quadrangles-Coatesville-West Chester folio: U. S. Geological Survey Geological Atlas of the United States, Folio 223, 15 p. with maps, scale 1:62,500.

Blackmer, G.C., 2005, Preliminary bedrock geologic map of a portion of the Wilmington 30- by 60-minute quadrangle, southeastern Pennsylvania: Pennsylvania Geological Survey, 4th ser., Open-File Report OFBM 05-01.0, 16 p.

Blackmer, G.C., Kunk, M.J., Southworth, S., and Bosbyshell, H., 2007, Timing of metamorphism and deformation in southeastern Pennsylvania and northern Delaware: Geological Society of America Abstracts with Programs, v. 39, no. 1, p. 75.

Bosbyshell, H., Blackmer, G.C., Srogi, L., Mathur, R., Crawford, M., Valencia, V., and Schenck, W.S., 2012, Detrital zircon ages from the Wissahickon Formation, southeast Pennsylvania and northern Delaware: Regional tectonic implications: Geological Society of America Abstracts with Programs, v. 44, no. 2, p. 87.

Bosbyshell, H., Blackmer, G.C., Mathur, R., Srogi, L., and Schenck, W.S., 2013, Significance of detrital zircon ages in the central Appalachian piedmont of southeastern Pennsylvania and Northern Delaware: Geological Society of America Abstracts with Programs, v. 45, no. 7, p. 810.

Bosbyshell, H., Blackmer, G.C., Schenck, W.S., and Srogi, L., 2014, Defining the West Grove Metamorphic Suite: Implications for Tectonic Interpretations of the Central Appalachian Piedmont, in de Wet, A.P., ed., Field Trip Guide, Northeastern Section of the Geological Society of America: Pennsylvania Geological Survey, p. 17–33. (This paper is available at http://www.geosociety.org/pubs/ft2015.htm as GSA Data Repository item 2015300.)

Bosbyshell, H., Srogi, L., Blackmer, G.C., Schenck, W.S., Mathur, R., and Valencia, V., 2015, The tectono-thermal evolution of the central Appalachian Orogen: Accretion of a peri-Gondwanan(?) Ordovician arc, in Brezinski, D.K., Halka, J.P., and Ortt, R.A., Jr., eds., Tripping from the Fall Line: Field Excursions for the GSA Annual Meeting, Baltimore, 2015: Geological Society of America Field Guide 40, p. 35.

Bosbyshell, H., Srogi, L., and Blackmer, G.C., 2016, Monazite age constraints on the tectono-thermal evolution of the central Appalachian Piedmont: American Mineralogist, v. 101, p. 1820–1838.

Chang, Z., Vervoort, J. D., McClelland, W.C., and Knaack, C., 2006, U-Pb dating of zircon by LA-ICP-MS: Geochemistry, Geophysics, Geosystems, vol. 7, no. 5.

Crowley, W.P., 1976, The geology of the crystalline rocks near Baltimore and its bearing on the evolution of the eastern Maryland Piedmont: Maryland Geological Survey Report of Investigations 27, 40 p.

Faill, R.T., 1997, A geologic history of the north-central Appalachians. Part I. Orogenesis from the Mesoproterozoic through the Taconic Orogeny: American Journal of Science, p. 551-619.

Higgins, M.W., 1990, The crystalline rocks of Cecil County, Maryland, in the geology of Cecil County, Maryland: Maryland Geological Survey Bulletin No. 37, p. 3-116.

Higgins, M.W., and Conant, L.B., 1986, Geologic map of Cecil County: Maryland Geological Survey County Geologic Map, scale 1:62,500.

Matthews, E.B., 1905, Correlation of Maryland and Pennsylvania Piedmont formations: Geological Society of America Bulletin, v. 16, p. 329-346.

Pavlides, L., 1974, Age, origin, regional relations, and nomenclature of the Glenarm Series, Central Appalachian Piedmont: a reinterpretation: Discussion: Geological Society of America Bulletin, v. 83, p. 153-155.

Plank, M.O., Schenck, W.S., and Srogi, L., 2000, Bedrock geology of the Piedmont of Delaware and adjacent Pennsylvania: Delaware Geological Survey, Report of Investigations No. 59, 52 p.

Plank, M.O., Srogi, L., Schenck, W.S., and Plank, T.A., 2001, Geochemistry of the Mafic Rocks, Delaware Piedmont and Adjacent Pennsylvania and Maryland: Confirmation of Arc Affinity: Delaware Geological Survey, Report of Investigations No. 60, 39 p.

Schenck, W.S., Plank, M.O., and Srogi, L., 2000, Bedrock geologic map of the Piedmont of Delaware and adjacent Pennsylvania: Delaware Geological Survey, Geologic Map Series No. 10, scale 1:36,000.

Schenck, W.S., 1997, Stratigraphic classification and nomenclature of the rocks in the Delaware Piedmont: Newark, Delaware, University of Delaware, unpublished MS. thesis, 106 p.

Smith, II, R.C., 2004, Bald Friar Metabasalt and Kennett Square Amphibolite: Two Iapetan ocean floor basalts, in Blackmer, G. C., and Srogi, L., eds., Marginalia – Magmatic arcs and continental margins in Delaware and southeastern Pennsylvania: Guidebook, 69th Annual Field Conference of Pennsylvania Geologists, West Chester, PA, p. 46-55.

Smith, II, R.C., and Barnes, J.H., 2004, White Clay Creek Amphibolite: A Piedmont analog of the Catoctin Metabasalt, in Blackmer, G.C., and Srogi, L., eds., Marginalia – Magmatic arcs and continental margins in Delaware and southeastern Pennsylvania: Guidebook, 69th Annual Field Conference of Pennsylvania Geologists, West Chester, PA, p. 28-45.

Valentino, D.W., Gates, A.E., and Glover, L., III, 1994, Late Paleozoic transcurrent tectonic assembly of the central Appalachian Piedmont: Tectonics, v. 13, p. 110-126.

Valentino, D.W., Valentino, R.W., and Hill, M.L., 1995, Paleozoic transcurrent conjugate shear zones in the Central Appalachian Piedmont of southeastern Pennsylvania: Journal of Geodynamics, v. 19, p. 303–324, doi:10.1016/0264-3707(94)00020-V.

Valentino, D.W., and Gates, A.E., 2001, Asynchronous extensional collapse of a transpressional orogen: the Alleghenian Central Appalachian Piedmont, USA: Journal of Geodynamics, v. 31, p. 145–167, doi:10.1016/S0264-3707(00)00028-4.

Wade, J.A., Plank, T., Stern, R.J., Tollstrup, D.L., Gill, J.B., O'Leary, J.C., Eiler, J.M., Moore, R.B., Woodhead, J.D., Trusdell, F. and Fischer, T.P., 2005. The May 2003 eruption of Anatahan volcano, Mariana Islands: Geochemical evolution of a silicic island-arc volcano.Journal of Volcanology and Geothermal Research, 146(1-3), pp.139-170.

Woodruff, K.D., and Thompson, A.M., 1972 (issued 1975), Geology of the Newark area, Delaware: Delaware Geological Survey Geologic Map Series No. 3, scale 1:24,000.

_________1975, Geology of the Wilmington area, Delaware: Delaware Geological Survey Geologic Map Series No. 4, scale 1:24,000.

APPENDIX 1

Geochemical Data for Canby Park, Windy Hills Gneiss, and Rockford Park Gneiss Mafic Layers. Analysis for the Canby Park Sample (Cc15-b) is new data, while Windy (Cb42-c) and Rockford (Bb41-b) are from published data in Plank et al. 2001. Analysis was performed at the Lamont Doherty Earth Observatory by Inductively Coupled Plasma-Mass Spectrometry (ICP-MS) and ICP-Emission Spectroscopy following HF: HNO_3 digestions, using methods in Wade et al. (2005). Oxides are in wt%, while elements are in wt ppm.

Sample	DGSID	DGS Sample No.	SiO[2] (by diff)	TiO[2]	Al[2]O[3]	Fe[2]O[3]	FeO	MgO	MnO	CaO	K[2]O	Na[2]O	P[2]O[5]	H2O -(120C)	LOI	Sr	Rb	Nb	Cs	Ba	Sc	V	Co	Ni	Cu	Y	Zr	Ga	Zn	La	Ce	Pr
WINDY	Cb42-c	43425	49.33	0.77	15.84	9.98	8.98	8.27	0.19	11.45	0.98		0.06	0.04	0.4	131.08	20.17	1.96	0.52	90.51	38.56	251.31	40.92	79.42	5.52	16.5		15.1	79.44	3.98	8.8	1.36
CANBY	Cc15-b	115775	48.8	0.83	15.26	9.74		9.3	0.17	11.92	0.82	3.12	0.06			127.75	5.65	1.55		100.86	38.56	232.94	46.72	170.62	5.21	21.14	48.77	15.31	73.44	3.03	7.73	1.29
ROCKFORD	Bd41-b	43428	49.4	0.33	17.05	10.78	9.7	7.52	0.17	11.55	0.4	2.53	0.02	0.07	0.17	92.4	2.82	1.42	0.06	78	41.6	308.71	39.8	56.87	5.35	6.23		14.27	79	2.35	5.43	0.7

Sample	DGSID	DGS Sample No.	Nd	U	Li	Be	Cr	Sm	Th	Eu	Gd	Tb	Dy	Ho	Er	Yb	Lu	Hf	Ta	Pb	U/Th	Zr/Hf	Ba/La	Y/Yb	La/Sm	Yb/Sm	La/Lu	La/Lu ratio	La conc.	La/Nb	Ti, ppm	Mg#	Alt Index
WINDY	Cb42-c	43425	6.26	0.18			315.8	1.85	0.39	0.81	2.95	0.53	3.44	0.75	2.12	2.06	0.32		0.1	2.3					2.16	0.88	15.55	1.6	12.8	2.04	4610	62.12	39.52
CANBY	Cc15-b	115775	6.43	0.15	0.83	0.8	434.7	2.18	0.44	0.72	2.42	0.42	2.7	0.59	1.66	1.62	0.26	1.32	0.3	2.79	0.34	37.11	33.85	10.44	1.39						4960		
ROCKFORD	Bd41-b	43428	2.8	0.07			248.9	0.73	0.32	0.29	0.86	0.15	0.99	0.22	0.65	0.72	0.12		0.07	3.24					3.23	0.98	19.72	2	7.55	1.65	1966	58	35.99

APPENDIX 2

Igneous Age of Crystallization Zircon Analysis for James Run Big Elk Sample (DGS Outcrop Zz63-ak, sample 117893)
Zircon analysis was performed by Ryan Mathur of Juniata College.

				Isotopic Ratios									AGES							
Running Name	Sample Name	U ppm	U/Th	^{207}Pb / ^{235}U	2σ Abs Error	^{206}Pb / ^{238}U	2σ Abs Error	Corr. Coef	^{238}U / ^{206}Pb	2σ Abs Error	^{207}Pb / ^{206}Pb	2σ Abs Error	^{207}Pb / ^{235}U Ma	2σ Abs Error Ma	^{206}Pb / ^{238}U Ma	2σ Abs Error Ma	^{207}Pb / ^{206}Pb Ma	2σ Abs Error Ma	Best Age Ma	2σ Abs Error Ma
RM_1	RYANMATHUR_1	332.1	1.1	0.5940	0.0130	0.0737	0.0009	0.2254	13.5318	0.1685	0.0585	0.0013	473.7	8.2	458.3	5.6	530.0	49.0	458.3	5.6
RM_2	RYANMATHUR_2	169.8	2.5	0.5905	0.0130	0.0745	0.0010	0.2995	13.3994	0.1742	0.0575	0.0014	471.5	8.5	463.3	6.0	486.0	52.0	463.3	6.0
RM_3	RYANMATHUR_3	689.0	8.8	0.5513	0.0087	0.0718	0.0008	0.4012	13.9295	0.1494	0.0557	0.0009	446.1	5.7	447.0	4.7	428.0	34.0	447.0	4.7
RM_4	RYANMATHUR_4	341.5	2.9	0.6101	0.0120	0.0771	0.0011	0.2798	12.9534	0.1846	0.0574	0.0012	483.9	7.6	479.0	6.7	484.0	48.0	479.0	6.7
RM_5	RYANMATHUR_5	631.8	1.5	2.2415	0.0350	0.2023	0.0024	0.4165	4.9383	0.0585	0.0804	0.0012	1194.9	11.0	1187.6	13.8	1199.0	30.0	1187.6	13.8
RM_6	RYANMATHUR_6	159.4	1.6	0.6142	0.0140	0.0771	0.0009	0.3928	12.9500	0.1526	0.0578	0.0012	486.5	8.8	478.8	5.6	497.0	48.0	478.8	5.6
RM_7	RYANMATHUR_7	1490.0	21.6	0.5374	0.0120	0.0706	0.0014	0.5584	14.1643	0.2809	0.0552	0.0011	437.0	7.8	440.0	8.6	407.0	43.0	440.0	8.6
RM_8	RYANMATHUR_8	209.0	1.3	0.5985	0.0130	0.0771	0.0010	0.4233	12.9702	0.1682	0.0563	0.0011	476.6	8.2	479.0	6.1	442.0	44.0	479.0	6.1
RM_9	RYANMATHUR_9	561.0	3.8	1.5728	0.0300	0.1538	0.0022	0.3546	6.4641	0.0919	0.0742	0.0015	960.1	12.0	922.3	12.8	1036.0	41.0	922.3	12.8
RM_10	RYANMATHUR_10	144.8	1.0	2.1597	0.0530	0.1979	0.0029	0.5517	5.0505	0.0740	0.0792	0.0017	1168.9	17.0	1163.8	16.7	1176.0	39.0	1163.8	16.7
RM_11	RYANMATHUR_11	385.2	1.2	0.6241	0.0110	0.0782	0.0009	0.3594	12.7632	0.1385	0.0579	0.0009	492.7	6.9	485.6	5.2	515.0	35.0	485.6	5.2
RM_12	RYANMATHUR_12	569.0	5.6	0.5442	0.0082	0.0699	0.0007	0.3044	14.2857	0.1469	0.0565	0.0009	441.5	5.2	435.7	4.4	465.0	32.0	435.7	4.4
RM_13	RYANMATHUR_13	341.0	5.8	0.5791	0.0110	0.0744	0.0011	0.3609	13.4409	0.1987	0.0565	0.0011	464.2	6.9	462.5	6.7	456.0	42.0	462.5	6.7
RM_14	RYANMATHUR_14	213.2	1.3	0.6346	0.0190	0.0769	0.0012	0.3705	12.9534	0.2013	0.0599	0.0017	499.3	12.0	477.4	7.3	576.0	61.0	477.4	7.3
RM_15	RYANMATHUR_15	601.0	1.6	0.5875	0.0120	0.0768	0.0011	0.3439	13.0378	0.1870	0.0555	0.0012	469.6	7.7	477.1	6.7	424.0	49.0	477.1	6.7
RM_16	RYANMATHUR_16	1257.0	15.7	0.5243	0.0070	0.0685	0.0008	0.4620	14.5922	0.1661	0.0555	0.0007	428.3	4.6	427.2	4.8	422.0	29.0	427.2	4.8
RM_17	RYANMATHUR_17	173.2	1.5	2.8010	0.0440	0.1985	0.0027	0.4467	4.8804	0.0643	0.1024	0.0016	1356.6	12.0	1167.1	15.1	1661.0	29.0	1661.0	29.0
RM_18	RYANMATHUR_18	485.0	0.8	0.5864	0.0110	0.0745	0.0011	0.3947	13.4048	0.1977	0.0571	0.0010	468.9	6.9	463.3	6.7	481.0	41.0	463.3	6.7
RM_19	RYANMATHUR_19	771.0	0.8	0.6176	0.0120	0.0771	0.0011	0.5716	12.9534	0.1846	0.0582	0.0009	488.6	7.5	478.5	6.7	529.0	35.0	478.5	6.7
RM_20	RYANMATHUR_20	454.0	1.4	0.5851	0.0096	0.0752	0.0010	0.4247	13.2908	0.1731	0.0564	0.0009	468.0	6.2	467.6	6.0	460.0	34.0	467.6	6.0
RM_21	RYANMATHUR_21	848.0	1.6	0.6134	0.0110	0.0775	0.0011	0.3555	12.8866	0.1827	0.0574	0.0011	486.0	6.8	481.4	6.7	490.0	40.0	481.4	6.7
RM_22	RYANMATHUR_22	561.4	1.4	0.5861	0.0110	0.0747	0.0012	0.5116	13.3690	0.2145	0.0569	0.0011	468.7	7.1	464.7	7.3	477.0	40.0	464.7	7.3
RM_23	RYANMATHUR_23	567.0	1.2	0.5738	0.0120	0.0742	0.0010	0.4044	13.4771	0.1816	0.0561	0.0010	460.7	7.6	461.5	6.1	453.0	42.0	461.5	6.1
RM_24	RYANMATHUR_24	261.5	2.0	0.6011	0.0130	0.0773	0.0013	0.4425	12.9366	0.2176	0.0564	0.0011	478.2	8.0	480.2	7.9	454.0	45.0	480.2	7.9
RM_25	RYANMATHUR_25	187.4	1.2	0.5818	0.0140	0.0751	0.0012	0.3849	13.3156	0.2128	0.0562	0.0013	465.9	9.2	466.9	7.3	443.0	52.0	466.9	7.3
RM_26	RYANMATHUR_26	685.0	2.0	2.0958	0.0330	0.1937	0.0027	0.4967	5.1573	0.0718	0.0785	0.0012	1148.1	11.0	1141.5	15.5	1153.0	30.0	1141.5	15.5
RM_29	RYANMATHUR_29	438.0	1.9	0.6056	0.0160	0.0770	0.0016	0.3292	12.9870	0.2699	0.0571	0.0013	481.1	9.8	477.9	9.8	473.0	51.0	477.9	9.8
RM_30	RYANMATHUR_30	508.0	6.6	0.5398	0.0077	0.0695	0.0005	0.2424	14.3761	0.1095	0.0564	0.0008	438.6	5.1	433.0	3.3	457.0	32.0	433.0	3.3
RM_31	RYANMATHUR_31	264.2	1.2	0.5835	0.0120	0.0739	0.0013	0.5682	13.5135	0.2374	0.0573	0.0010	467.0	8.0	459.6	7.9	492.0	41.0	459.6	7.9
RM_32	RYANMATHUR_32	226.5	2.2	0.5703	0.0170	0.0740	0.0018	0.3082	13.5135	0.3287	0.0559	0.0019	458.5	11.0	460.4	11.0	430.0	73.0	460.4	11.0
RM_33	RYANMATHUR_33	407.0	2.3	2.1246	0.0530	0.1818	0.0048	0.5444	5.4318	0.1416	0.0848	0.0021	1157.5	17.0	1076.7	27.4	1300.0	50.0	1076.7	27.4
RM_34	RYANMATHUR_34	512.0	1.6	0.5769	0.0099	0.0748	0.0010	0.4316	13.3690	0.1787	0.0559	0.0009	462.7	6.4	465.2	6.1	438.0	38.0	465.2	6.1
RM_35	RYANMATHUR_35	34.8	1.4	2.5595	0.0490	0.2219	0.0036	0.2255	4.5086	0.0732	0.0837	0.0019	1289.9	14.0	1291.8	20.6	1272.0	43.0	1291.8	20.6
RM_36	RYANMATHUR_36	114.4	1.5	0.6060	0.0130	0.0773	0.0011	0.3181	12.9366	0.1841	0.0569	0.0013	481.3	8.0	479.9	6.7	461.0	48.0	479.9	6.7
RM_37	RYANMATHUR_37	271.0	3.8	0.5814	0.0097	0.0745	0.0012	0.4565	13.4228	0.2162	0.0567	0.0010	465.6	6.2	463.0	7.3	460.0	38.0	463.0	7.3
RM_38	RYANMATHUR_38	133.7	2.6	0.6169	0.0120	0.0766	0.0009	0.2927	13.0174	0.1576	0.0584	0.0011	488.2	7.7	476.0	5.7	528.0	44.0	476.0	5.7

				Isotopic Ratios									AGES							
Running Name	Sample Name	U ppm	U/Th	^{207}Pb / ^{235}U	2σ Abs Error	^{206}Pb /^{238}U	2σ Abs Error	Corr. Coef	^{238}U / ^{206}Pb	2σ Abs Error	^{207}Pb / ^{206}Pb	2σ Abs Error	^{207}Pb / ^{235}U Ma	2σ Abs Error Ma	^{206}Pb / ^{238}U Ma	2σ Abs Error Ma	^{207}Pb / ^{206}Pb Ma	2σ Abs Error Ma	Best Age Ma	2σ Abs Error Ma
RM_39	RYANMATHUR_39	302.0	7.5	0.5367	0.0093	0.0701	0.0010	0.4378	14.2653	0.2035	0.0556	0.0010	436.5	6.2	436.8	6.1	416.0	38.0	436.8	6.1
RM_40	RYANMATHUR_40	216.0	1.3	0.5996	0.0100	0.0769	0.0011	0.4572	13.0039	0.1860	0.0566	0.0010	477.3	6.7	477.6	6.7	461.0	37.0	477.6	6.7
RM_41	RYANMATHUR_41	147.2	4.2	1.2143	0.0260	0.1225	0.0019	0.5498	8.0775	0.1240	0.0719	0.0013	807.7	12.0	745.2	11.2	973.0	38.0	745.2	11.2
RM_42	RYANMATHUR_42	92.6	3.2	1.9069	0.0380	0.1797	0.0033	0.4497	5.5494	0.1016	0.0770	0.0016	1084.2	14.0	1065.3	19.0	1107.0	42.0	1065.3	19.0
RM_43	RYANMATHUR_43	166.0	1.1	0.5845	0.0110	0.0745	0.0010	0.4217	13.4048	0.1797	0.0569	0.0010	467.7	6.8	463.5	6.1	479.0	40.0	463.5	6.1
RM_44	RYANMATHUR_44	278.1	1.5	0.5772	0.0098	0.0740	0.0009	0.4266	13.5007	0.1713	0.0566	0.0009	462.9	6.3	460.4	5.7	463.0	34.0	460.4	5.7
RM_45	RYANMATHUR_45	216.6	2.2	0.5782	0.0093	0.0742	0.0008	0.3442	13.4716	0.1452	0.0565	0.0009	463.6	5.9	461.4	4.9	459.0	35.0	461.4	4.9
RM_46	RYANMATHUR_46	101.8	1.7	0.5858	0.0130	0.0743	0.0011	0.5373	13.4409	0.1987	0.0572	0.0011	468.5	8.3	462.1	6.7	487.0	42.0	462.1	6.7
RM_47	RYANMATHUR_47	512.0	1.2	0.5786	0.0088	0.0739	0.0009	0.4849	13.5263	0.1610	0.0568	0.0008	463.9	5.6	459.4	5.4	477.0	30.0	459.4	5.4
RM_50	RYANMATHUR_50	331.0	1.6	0.6328	0.0220	0.0750	0.0017	0.5913	13.2450	0.2982	0.0612	0.0016	498.2	14.0	466.4	10.3	629.0	60.0	466.4	10.3
RM_51	RYANMATHUR_51	173.0	1.4	0.5979	0.0120	0.0765	0.0009	0.4663	13.0668	0.1588	0.0567	0.0010	476.2	7.7	475.3	5.7	462.0	40.0	475.3	5.7
RM_52	RYANMATHUR_52	243.0	0.9	0.5892	0.0087	0.0753	0.0009	0.4192	13.2679	0.1584	0.0568	0.0009	470.7	5.6	468.2	5.5	472.0	33.0	468.2	5.5
RM_53	RYANMATHUR_53	80.1	1.0	0.5715	0.0120	0.0750	0.0009	0.1738	13.3547	0.1676	0.0553	0.0012	459.2	7.4	466.1	5.8	408.0	48.0	466.1	5.8
RM_54	RYANMATHUR_54	46.0	2.4	0.6108	0.0150	0.0767	0.0013	0.2911	13.0208	0.2204	0.0578	0.0014	484.4	9.6	476.3	7.9	510.0	55.0	476.3	7.9
RM_56	RYANMATHUR_56	507.0	1.3	0.6083	0.0090	0.0778	0.0009	0.5210	12.8485	0.1519	0.0567	0.0007	482.8	5.6	483.2	5.6	473.0	29.0	483.2	5.6
RM_57	RYANMATHUR_57	93.5	1.2	0.6113	0.0120	0.0763	0.0009	0.2975	13.0736	0.1487	0.0581	0.0011	484.6	7.5	474.2	5.3	519.0	42.0	474.2	5.3
RM_58	RYANMATHUR_58	66.8	1.1	0.5973	0.0130	0.0773	0.0011	0.1961	12.9534	0.1846	0.0561	0.0013	475.8	8.1	479.7	6.7	430.0	51.0	479.7	6.7
RM_59	RYANMATHUR_59	154.0	1.2	1.7906	0.0210	0.1774	0.0018	0.4439	5.6465	0.0574	0.0733	0.0009	1042.7	7.7	1052.6	10.4	1013.0	24.0	1052.6	10.4
RM_60	RYANMATHUR_60	54.9	0.6	1.7781	0.0270	0.1748	0.0023	0.3436	5.7208	0.0753	0.0738	0.0012	1038.1	10.0	1038.6	13.3	1021.0	33.0	1038.6	13.3

DGSID	Location	Northing *UTM-18m*	Easting *UTM-18m*	Lithology
Zz63-ak	James Run Big Elk Member, Fair Hill, MD	4395163.2	428487.8	mafic-felsic gneiss

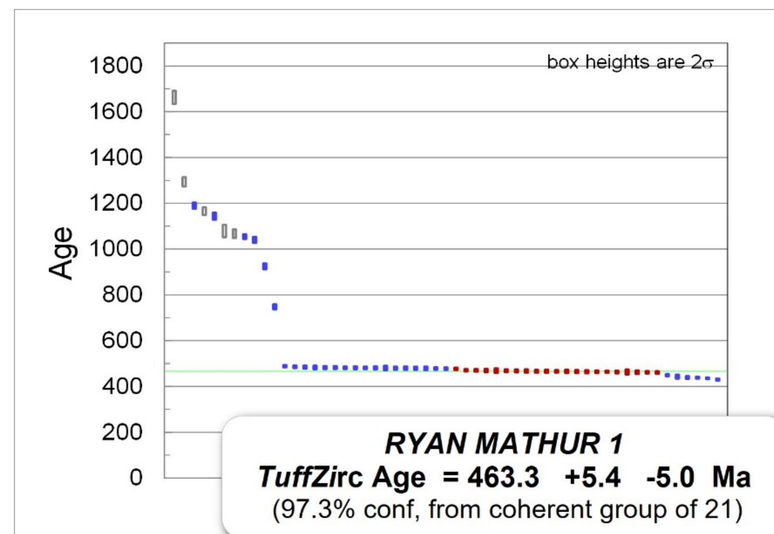

APPENDIX 3

Detrital Zircon Analysis for Thompsons Bridge Gneiss (DGS Outcrops Bc54-g, sample 100579; Cb42-d, sample 113500; and Bd21-j, sample 113469).

Detrital zircon analysis was performed by Ryan Mathur of Juniata College. For each of the three samples, 1-1.5 kg worth of rock was processed, and zircon was separated using standard heavy liquid gravimetric and magnetic separation techniques. Extracted zircons and standards were mounted on a 1-inch diameter epoxy puck that was ground and polished to expose the grains (Chang et al 2006). Photomicrograph maps and cathodoluminescence (CL) illustrated laser spot locations and revealed growth zones and inclusions within the zircon crystals, respectively. LA-ICP-MS U-Pb zircon work was performed using a New Wave UP-213 laser ablation system in conjunction with a Thermo Finnigan Element2 single collector double focusing magnetic sector ICPMS in the GeoAnalytical Lab at Washington State University. Analytical procedures for zircon dating followed methods fully described in Chang et al (2006). Results from grains with >20% normal discordance, >5% reverse discordance, or >10% measurement (internal) uncertainty were not included. $^{206}Pb/^{238}U$ dates were used for grains with $^{206}Pb/^{207}Pb$ dates younger than 900 Ma and $^{206}Pb/^{207}Pb$ dates for older grains.

sample name	U	Th/U	238U/206Pb	1 sigma	207Pb/206Pb	1 sigma	206Pb/238U	+/- 1σ	207Pb/206Pb	+/- 1σ	Best age	+/- 1σ
	ppm			% error		% error	age	Ma	age	Ma	Ma	Ma
Cb42-d_a_1	80	0.5	3.1040	2.0	0.1147	0.9	1800	32	1875	15	1875	15
Cb42-d_a_2	426	0.3	5.4531	1.9	0.0769	0.8	1085	19	1118	16	1118	16
Cb42-d_a_3	373	0.3	4.8919	1.9	0.0816	0.8	1199	21	1237	16	1237	16
Cb42-d_a_4	156	0.5	4.9922	2.0	0.0810	0.9	1177	21	1221	17	1221	17
Cb42-d_a_5	158	0.4	3.8291	1.9	0.0939	0.9	1496	25	1506	17	1506	17
Cb42-d_a_6	87	0.5	5.4850	2.1	0.0797	1.2	1080	21	1189	23	1189	23
Cb42-d_a_7	59	0.6	10.5377	2.1	0.0603	1.9	584	12	613	41	584	12
Cb42-d_a_8	211	0.3	5.1639	2.0	0.0805	0.8	1141	21	1209	16	1209	16
Cb42-d_a_10	332	0.7	5.7169	2.0	0.0759	0.8	1039	19	1093	16	1093	16
Cb42-d_a_11	119	0.7	5.7395	2.1	0.0761	1.3	1035	20	1099	25	1099	25
Cb42-d_a_12	465	0.5	4.9748	2.0	0.0809	0.7	1181	21	1219	14	1219	14
Cb42-d_a_13	52	1.0	5.9270	2.1	0.0717	1.4	1005	20	978	28	978	28
Cb42-d_a_14	50	0.7	4.5243	2.0	0.0845	1.5	1287	24	1305	29	1305	29
Cb42-d_a_15	426	0.4	4.9880	1.9	0.0804	0.8	1178	21	1207	15	1207	15
Cb42-d_a_16	263	0.4	3.9283	1.9	0.0947	0.7	1462	25	1523	14	1523	14
Cb42-d_a_17	48	0.4	5.7994	2.1	0.0745	1.4	1026	20	1056	29	1056	29
Cb42-d_a_18	98	0.2	5.9148	2.1	0.0755	1.1	1007	19	1083	22	1083	22
Cb42-d_a_19	227	0.4	5.6341	2.0	0.0762	0.9	1053	19	1101	18	1101	18
Cb42-d_a_21	79	0.4	4.2940	2.2	0.0874	1.1	1350	26	1369	21	1369	21

sample name	U	Th/U	238U/206Pb	1 sigma	207Pb/206Pb	1 sigma	206Pb/238U	+/- 1σ	207Pb/206Pb	+/- 1σ	Best age	+/- 1σ
	ppm			% error		% error	age	Ma	age	Ma	Ma	Ma
Cb42-d_a_22	98	0.5	4.6866	2.1	0.0823	1.0	1247	23	1253	20	1253	20
Cb42-d_a_23	337	0.8	4.8867	2.0	0.0821	0.8	1200	22	1247	15	1247	15
Cb42-d_a_24	122	0.4	5.8446	2.0	0.0745	1.1	1018	19	1056	21	1056	21
Cb42-d_a_25	391	0.1	5.4196	2.0	0.0774	0.8	1092	20	1133	16	1133	16
Cb42-d_a_27	34	0.8	5.7850	2.2	0.0736	1.7	1028	21	1031	34	1031	34
Cb42-d_a_28	65	0.7	4.9429	2.1	0.0804	1.2	1188	23	1207	23	1207	23
Cb42-d_a_29	139	0.3	3.9083	2.2	0.0932	0.9	1469	28	1491	18	1491	18
Cb42-d_a_30	90	0.3	4.7440	2.0	0.0833	1.1	1233	22	1276	21	1276	21
Cb42-d_a_31	152	0.7	3.8097	2.0	0.0942	0.8	1503	26	1512	16	1512	16
Cb42-d_a_32	214	0.4	4.8499	2.0	0.0805	0.9	1208	22	1208	17	1208	17
Cb42-d_a_33	369	0.2	3.1451	1.9	0.1107	0.7	1780	29	1811	13	1811	13
Cb42-d_a_34	130	0.5	6.2258	2.0	0.0741	1.0	960	18	1044	20	1044	20
Cb42-d_a_35	99	0.4	4.1190	2.0	0.0914	1.0	1401	26	1454	18	1454	18
Cb42-d_a_37	628	0.4	4.5504	1.9	0.0849	0.7	1281	22	1314	14	1314	14
Cb42-d_a_38	1176	0.2	6.0503	1.9	0.0730	0.7	986	17	1014	14	1014	14
Cb42-d_a_39	31	0.6	4.9159	2.3	0.0816	1.4	1194	25	1237	28	1237	28
Cb42-d_a_40	363	0.9	4.2679	1.9	0.0885	0.8	1357	24	1393	15	1393	15
Cb42-d_a_41	575	0.6	5.4666	1.9	0.0798	0.7	1083	19	1191	14	1191	14
Cb42-d_a_42	779	0.5	4.4219	1.9	0.0870	0.7	1314	23	1360	14	1360	14
Cb42-d_a_43	44	0.7	5.1994	2.3	0.0806	1.4	1134	23	1211	26	1211	26
Cb42-d_a_44	167	0.3	3.9209	2.0	0.0933	0.8	1464	26	1494	15	1494	15
Cb42-d_a_45	132	0.3	3.8218	2.0	0.0956	1.0	1498	26	1540	19	1540	19
Cb42-d_a_46	201	0.3	5.4495	2.0	0.0770	1.0	1086	20	1122	19	1122	19
Cb42-d_a_47	195	0.4	5.1738	2.0	0.0804	0.9	1139	20	1207	17	1207	17
Cb42-d_a_48	103	0.4	4.6922	2.0	0.0801	1.1	1245	22	1199	21	1199	21
Cb42-d_a_49	252	0.3	5.3588	1.9	0.0780	0.9	1103	20	1146	17	1146	17
Cb42-d_a_50	302	0.3	5.1569	2.0	0.0817	0.9	1143	21	1238	18	1238	18
Cb42-d_a_51	414	0.4	4.8923	1.9	0.0810	0.8	1199	21	1222	16	1222	16
Cb42-d_a_52	198	1.2	5.8335	2.2	0.0747	1.0	1020	20	1062	20	1062	20
Cb42-d_a_53	133	0.9	5.5492	2.0	0.0793	1.0	1068	19	1180	20	1180	20
Cb42-d_a_55	338	0.4	6.0227	1.9	0.0722	0.8	990	17	991	16	991	16

sample name	U	Th/U	238U/206Pb	1 sigma	207Pb/206Pb	1 sigma	206Pb/238U	+/- 1σ	207Pb/206Pb	+/- 1σ	Best age	+/- 1σ
	ppm			% error		% error	age	Ma	age	Ma	Ma	Ma
Cb42-d_a_56	252	1.3	5.8117	1.9	0.0741	0.9	1023	18	1045	17	1045	17
Cb42-d_1	200	0.1	4.8529	1.7	0.0823	1.1	1208	18	1252	21	1252	21
Cb42-d_2	867	0.2	4.8990	1.7	0.0786	1.0	1197	18	1163	19	1163	19
Cb42-d_3	432	0.3	5.6455	1.7	0.0755	1.0	1051	17	1083	19	1083	19
Cb42-d_4	120	1.2	10.4843	1.9	0.0594	1.5	587	11	583	32	587	11
Cb42-d_5	799	0.2	5.0309	1.7	0.0790	0.9	1169	18	1172	18	1172	18
Cb42-d_6	177	0.4	6.3385	1.8	0.0717	1.2	944	16	978	24	978	24
Cb42-d_7	153	0.9	2.4972	1.9	0.1535	1.0	2171	34	2386	16	2386	16
Cb42-d_8	243	0.4	5.2458	1.9	0.0756	1.1	1125	19	1086	22	1086	22
Cb42-d_9	63	0.5	3.8285	2.0	0.0934	1.3	1496	26	1496	25	1496	25
Cb42-d_11	76	0.5	5.4971	1.8	0.0771	1.4	1077	18	1124	28	1124	28
Cb42-d_12	203	0.3	5.4283	1.8	0.0769	1.4	1090	18	1118	28	1118	28
Cb42-d_13	1509	0.4	4.4412	1.6	0.0865	0.9	1309	19	1349	17	1349	17
Cb42-d_14	291	0.4	5.0629	1.9	0.0778	1.0	1162	20	1141	20	1141	20
Cb42-d_15	130	0.1	5.4823	1.7	0.0741	1.2	1080	17	1046	24	1046	24
Cb42-d_16	95	0.5	4.6787	1.7	0.0827	1.2	1249	20	1262	24	1262	24
Cb42-d_17	349	0.2	5.7143	1.7	0.0735	1.1	1040	16	1029	21	1029	21
Cb42-d_18	160	0.3	6.0637	1.7	0.0724	1.2	984	16	997	23	997	23
Cb42-d_20	322	0.3	6.4439	1.7	0.0715	1.0	930	15	972	21	972	21
Cb42-d_21	464	0.0	5.8207	1.6	0.0744	1.0	1022	15	1053	20	1053	20
Cb42-d_22	183	0.8	3.5928	1.6	0.0995	1.0	1583	22	1615	19	1615	19
Cb42-d_23	498	0.4	5.6647	1.9	0.0767	1.2	1048	19	1112	23	1112	23
Cb42-d_24	413	0.2	5.8997	2.6	0.0761	1.4	1009	24	1097	27	1097	27
Cb42-d_26	346	0.4	4.6937	1.9	0.0789	1.1	1245	21	1170	22	1170	22
Cb42-d_28	172	0.6	4.8665	1.7	0.0806	1.0	1205	19	1211	20	1211	20
Cb42-d_30	107	0.5	5.5235	1.8	0.0759	1.4	1073	18	1093	28	1093	28
Cb42-d_31	164	0.5	8.9688	1.9	0.0628	1.4	681	12	703	30	681	12
Cb42-d_32	26	0.2	5.2155	2.5	0.0762	2.0	1131	26	1099	40	1099	40
Cb42-d_33	94	0.3	5.1358	1.9	0.0779	1.3	1147	20	1145	25	1145	25
Cb42-d_34	189	0.2	5.7297	1.8	0.0754	1.2	1037	17	1080	23	1080	23
Cb42-d_35	262	0.5	4.6549	1.9	0.0827	1.1	1254	22	1261	21	1261	21

sample name	U	Th/U	238U/206Pb	1 sigma	207Pb/206Pb	1 sigma	206Pb/238U	+/- 1σ	207Pb/206Pb	+/- 1σ	Best age	+/- 1σ
	ppm			% error		% error	age	Ma	age	Ma	Ma	Ma
Cb42-d_36	1058	0.2	5.7887	1.6	0.0728	0.9	1027	15	1010	19	1010	19
Cb42-d_37	77	0.3	4.7062	1.9	0.0838	1.3	1242	21	1288	25	1288	25
Cb42-d_38	117	0.7	3.7375	1.7	0.0985	1.1	1528	23	1597	21	1597	21
Cb42-d_39	160	0.5	5.2582	1.9	0.0781	1.1	1122	20	1150	22	1150	22
Cb42-d_40	152	0.3	4.3541	1.8	0.0860	1.1	1333	22	1338	21	1338	21
Cb42-d_41	205	0.6	5.0784	1.8	0.0784	1.0	1159	19	1158	21	1158	21
Cb42-d_42	56	1.1	3.9661	1.9	0.0900	1.3	1449	25	1426	25	1426	25
Cb42-d_43	60	0.4	4.9585	1.9	0.0797	1.5	1184	21	1189	29	1189	29
Cb42-d_44	48	0.5	4.7554	1.8	0.0836	1.5	1230	20	1283	29	1283	29
Cb42-d_45	642	0.2	12.0053	1.8	0.0590	1.1	516	9	566	23	516	9
Cb42-d_47	203	0.7	6.0614	1.7	0.0711	1.1	984	16	962	22	962	22
Cb42-d_48	100	0.9	4.5504	1.8	0.0854	1.1	1281	21	1324	21	1324	21
Cb42-d_49	467	0.3	5.1884	2.0	0.0784	1.1	1136	20	1157	21	1157	21
Cb42-d_50	29	0.7	6.3530	2.1	0.0691	2.0	942	18	903	41	903	41
Cb42-d_51	348	0.3	3.7174	1.6	0.0919	1.0	1536	22	1465	18	1465	18
Cb42-d_53	287	0.3	4.0213	1.7	0.0894	1.0	1432	21	1413	19	1413	19
Cb42-d_54	132	0.3	4.8999	1.7	0.0769	1.1	1197	19	1119	21	1119	21
Cb42-d_56	1128	0.3	5.4196	1.6	0.0753	0.9	1092	16	1076	18	1076	18
Cb42-d_57	59	0.4	5.1389	1.8	0.0783	1.3	1146	19	1155	26	1155	26
Cb42-d_59	260	0.4	4.8420	1.6	0.0816	1.0	1210	18	1237	20	1237	20
Cb42-d_60	292	0.5	4.6473	1.6	0.0842	1.1	1256	19	1297	21	1297	21
Cb42-d_61	116	0.5	4.9406	1.6	0.0814	1.1	1188	18	1231	22	1231	22
Cb42-d_62	103	0.9	5.2730	1.7	0.0768	1.2	1119	17	1116	25	1116	25
Cb42-d_63	142	0.0	14.5312	1.8	0.0555	1.4	429	8	434	32	429	8
Cb42-d_64	115	0.2	4.0935	1.7	0.0880	1.1	1409	21	1382	21	1382	21
Cb42-d_65	215	0.4	4.9695	1.7	0.0775	1.1	1182	18	1134	21	1134	21
Cb42-d_66	281	0.7	10.6129	1.7	0.0607	1.2	580	9	628	26	580	9
Cb42-d_67	243	0.3	5.3699	1.8	0.0745	1.0	1101	18	1054	21	1054	21
Cb42-d_68	130	1.0	3.8517	1.6	0.0922	1.0	1488	22	1471	19	1471	19
Cb42-d_69	186	0.4	5.5297	1.7	0.0778	1.1	1072	16	1142	21	1142	21
Cb42-d_70	287	0.9	3.3410	1.6	0.1010	1.0	1688	24	1642	18	1642	18

sample name	U	Th/U	238U/206Pb	1 sigma	207Pb/206Pb	1 sigma	206Pb/238U	+/- 1σ	207Pb/206Pb	+/- 1σ	Best age	+/- 1σ
	ppm			% error		% error	age	Ma	age	Ma	Ma	Ma
Cb42-d_71	137	0.4	3.7465	1.7	0.0916	1.0	1525	23	1458	19	1458	19
Cb42-d_72	225	0.4	5.2858	1.7	0.0790	1.0	1117	17	1173	20	1173	20
Cb42-d_73	101	0.3	5.7436	1.8	0.0718	1.3	1035	18	980	26	980	26
Cb42-d_74	185	0.4	4.2550	1.8	0.0862	1.1	1361	21	1344	21	1344	21
Cb42-d_75	345	0.7	4.9923	1.8	0.0836	1.1	1177	19	1284	22	1284	22
Cb42-d_76	71	0.2	5.3883	2.0	0.0762	1.4	1097	20	1099	29	1099	29
Cb42-d_77	93	0.4	5.5245	1.8	0.0789	1.2	1073	18	1171	24	1171	24
Cb42-d_78	325	0.3	3.9327	1.7	0.0911	1.0	1460	22	1448	19	1448	19
Cb42-d_80	559	0.4	4.6807	1.8	0.0831	1.0	1248	20	1273	19	1273	19
Cb42-d_81	193	0.5	5.6814	1.7	0.0758	1.1	1045	17	1090	21	1090	21
Cb42-d_82	542	0.1	6.1290	1.7	0.0745	0.9	974	16	1054	19	1054	19
Cb42-d_83	103	0.6	4.3311	1.8	0.0872	1.2	1339	21	1364	23	1364	23
Cb42-d_84	237	0.4	4.0261	1.8	0.0930	1.1	1430	23	1489	20	1489	20
Cb42-d_85	486	0.7	5.7624	2.1	0.0735	1.0	1032	20	1027	19	1027	19
Cb42-d_86	243	0.3	5.1834	2.1	0.0789	1.1	1137	21	1170	21	1170	21
Cb42-d_87	142	0.4	5.1412	1.9	0.0776	1.2	1146	20	1137	23	1137	23
Cb42-d_88	236	0.5	5.1998	2.1	0.0787	1.1	1134	22	1164	22	1164	22
Cb42-d_89	47	0.4	5.2996	2.1	0.0795	1.2	1114	22	1185	24	1185	24
Bc54-g-100579_113	647	0.5	4.4714	1.7	0.0863	0.5	1301	20	1346	10	1346	10
Bc54-g-100579_112	590	0.4	4.2002	1.6	0.0865	0.5	1377	20	1350	11	1350	11
Bc54-g-100579_110	115	0.3	4.7760	1.7	0.0825	0.7	1226	19	1257	14	1257	14
Bc54-g-100579_109	198	0.4	4.5945	1.7	0.0828	0.6	1269	20	1265	12	1265	12
Bc54-g-100579_108	203	0.5	4.1699	1.6	0.0881	0.6	1386	20	1385	12	1385	12
Bc54-g-100579_107	52	0.4	3.9591	1.7	0.0925	0.9	1452	23	1478	16	1478	16
Bc54-g-100579_106	38	0.3	4.4373	1.9	0.0895	0.9	1310	22	1415	18	1310	22
Bc54-g-100579_105	355	0.9	4.9751	1.6	0.0786	0.6	1181	18	1163	12	1163	12
Bc54-g-100579_104	455	0.7	4.2108	1.7	0.0915	0.5	1374	21	1458	10	1458	10
Bc54-g-100579_103	392	0.2	4.8422	1.7	0.0834	0.6	1210	19	1279	12	1279	12
Bc54-g-100579_102	659	0.3	5.2885	1.6	0.0753	0.6	1116	17	1077	11	1077	11
Bc54-g-100579_101	176	0.4	4.9420	1.7	0.0799	0.6	1188	19	1194	12	1194	12
Bc54-g-100579_100	133	0.4	5.9620	1.8	0.0753	0.7	1000	16	1077	14	1077	14

sample name	U	Th/U	238U/206Pb	1 sigma	207Pb/206Pb	1 sigma	206Pb/238U	+/- 1σ	207Pb/206Pb	+/- 1σ	Best age	+/- 1σ
	ppm			% error		% error	age	Ma	age	Ma	Ma	Ma
Bc54-g-100579_98	1851	0.2	5.1731	2.4	0.0789	0.5	1139	25	1170	11	1170	11
Bc54-g-100579_97	905	0.1	5.6886	1.7	0.0730	0.6	1044	16	1015	12	1015	12
Bc54-g-100579_96	905	0.3	5.0561	1.6	0.0783	0.5	1163	17	1155	10	1155	10
Bc54-g-100579_95	330	0.4	6.3687	1.7	0.0728	0.6	940	15	1009	12	940	15
Bc54-g-100579_93	583	0.9	3.7985	1.7	0.0930	0.6	1507	23	1487	10	1487	10
Bc54-g-100579_92	78	0.6	5.6439	1.8	0.0737	1.1	1052	18	1033	23	1033	23
Bc54-g-100579_91	492	0.5	4.9390	1.7	0.0776	0.9	1189	19	1136	17	1136	17
Bc54-g-100579_90	100	0.4	8.6877	1.9	0.0627	1.1	702	12	699	24	702	12
Bc54-g-100579_89	433	0.5	4.8726	1.7	0.0793	0.8	1203	18	1179	16	1179	16
Bc54-g-100579_87	397	0.4	4.5826	1.7	0.0828	0.8	1272	19	1265	17	1265	17
Bc54-g-100579_86	112	0.8	6.3281	1.8	0.0703	1.1	946	16	938	22	946	16
Bc54-g-100579_85	1938	0.3	5.7415	1.9	0.0722	0.8	1035	18	992	17	992	17
Bc54-g-100579_84	112	0.8	6.3281	1.8	0.0703	1.1	946	16	938	22	946	16
Bc54-g-100579_83	139	1.2	5.9455	1.7	0.0729	1.0	1002	16	1011	19	1011	19
Bc54-g-100579_80	1261	0.5	5.0154	1.7	0.0780	0.8	1172	18	1147	16	1147	16
Bc54-g-100579_79	261	0.2	5.0700	1.7	0.0754	0.9	1160	18	1078	17	1078	17
Bc54-g-100579_78	644	0.4	3.9350	1.7	0.0918	0.8	1460	22	1463	15	1460	22
Bc54-g-100579_77	254	1.0	5.4940	1.7	0.0758	0.9	1078	17	1090	17	1090	17
Bc54-g-100579_76	464	0.3	5.5697	1.7	0.0746	0.8	1064	16	1057	17	1057	17
Bc54-g-100579_75	172	0.4	5.4193	1.7	0.0785	0.9	1092	17	1159	18	1159	18
Bc54-g-100579_71	304	0.3	3.2433	1.7	0.1052	0.8	1732	26	1717	15	1717	15
Bc54-g-100579_70	821	1.0	6.2334	1.7	0.0741	0.8	959	15	1043	17	1043	17
Bc54-g-100579_69	159	0.6	4.1176	1.8	0.0904	0.9	1402	22	1435	17	1435	17
Bc54-g-100579_68	75	0.4	4.6705	1.8	0.0814	1.0	1251	20	1231	20	1231	20
Bc54-g-100579_67	213	0.3	5.3603	1.7	0.0771	0.9	1103	18	1125	18	1125	18
Bc54-g-100579_66	267	0.3	5.4350	1.9	0.0773	0.9	1089	19	1130	18	1130	18
Bc54-g-100579_65	242	0.4	4.7156	1.8	0.0822	0.9	1240	20	1249	17	1240	20
Bc54-g-100579_63	1571	0.2	4.8691	1.7	0.0783	0.8	1204	19	1153	16	1153	16
Bc54-g-100579_62	74	0.6	6.1037	1.7	0.0709	1.1	978	16	954	22	978	16
Bc54-g-100579_61	617	0.5	5.2583	2.1	0.0752	0.9	1122	21	1075	18	1075	18
Bc54-g-100579_60	930	0.6	4.7827	1.7	0.0828	1.0	1224	19	1264	20	1264	20

sample name	U	Th/U	238U/206Pb	1 sigma	207Pb/206Pb	1 sigma	206Pb/238U	+/- 1σ	207Pb/206Pb	+/- 1σ	Best age	+/- 1σ
	ppm			% error		% error	age	Ma	age	Ma	Ma	Ma
Bc54-g-100579_59	100	0.4	6.0992	2.0	0.0728	0.9	979	18	1007	19	979	18
Bc54-g-100579_58	641	1.1	5.1866	1.9	0.0793	0.6	1137	20	1181	13	1137	20
Bc54-g-100579_57	98	0.9	6.7001	2.0	0.0696	1.0	897	17	917	21	897	17
Bc54-g-100579_56	379	0.6	5.7482	1.9	0.0747	0.7	1034	18	1060	13	1060	13
Bc54-g-100579_55	764	0.6	4.2593	1.9	0.0872	0.6	1360	24	1366	12	1366	12
Bc54-g-100579_54	103	1.1	4.5651	2.0	0.0845	0.9	1277	24	1305	17	1305	17
Bc54-g-100579_53	527	0.4	5.1239	1.9	0.0789	0.6	1149	20	1170	13	1170	13
Bc54-g-100579_52	1163	0.5	5.2347	2.1	0.0778	0.6	1127	21	1142	12	1142	12
Bc54-g-100579_51	307	0.5	5.1965	2.0	0.0795	0.7	1135	21	1185	14	1185	14
Bc54-g-100579_50	201	0.7	3.9142	2.0	0.0917	0.7	1467	26	1461	13	1461	13
Bc54-g-100579_49	209	0.3	5.3201	2.0	0.0769	0.8	1110	21	1120	16	1120	16
Bc54-g-100579_48	220	0.9	4.4752	2.0	0.0882	0.7	1300	24	1388	13	1388	13
Bc54-g-100579_47	291	0.3	5.0569	1.9	0.0831	0.7	1163	20	1272	13	1272	13
Bc54-g-100579_46	209	0.3	4.2449	1.9	0.0872	0.7	1364	24	1366	14	1366	14
Bc54-g-100579_45	622	0.3	5.0116	1.9	0.0793	0.6	1173	21	1179	13	1179	13
Bc54-g-100579_44	1390	0.3	6.4533	1.9	0.0737	0.6	929	16	1034	13	929	16
Bc54-g-100579_43	1403	0.3	4.0908	2.4	0.0964	3.2	1410	30	1556	58	1556	58
Bc54-g-100579_42	81	0.5	5.8106	2.0	0.0743	0.9	1024	19	1049	19	1049	19
Bc54-g-100579_41	415	0.4	4.3547	2.0	0.0907	0.7	1333	24	1441	12	1441	12
Bc54-g-100579_40	108	0.4	5.6557	1.9	0.0758	0.9	1050	19	1091	17	1091	17
Bc54-g-100579_38	811	0.3	5.9996	1.9	0.0767	0.6	994	17	1113	13	1113	13
Bc54-g-100579_37	219	0.6	6.3175	1.9	0.0722	0.7	947	17	991	14	947	17
Bc54-g-100579_36	129	0.3	6.2848	2.0	0.0708	0.8	952	17	951	16	952	17
Bc54-g-100579_35	370	0.4	5.7121	2.1	0.0788	0.7	1040	20	1166	14	1166	14
Bc54-g-100579_34	378	0.4	5.0852	1.9	0.0799	0.7	1157	20	1194	13	1194	13
Bc54-g-100579_33	585	0.4	6.1277	2.0	0.0720	0.6	974	18	985	13	974	18
Bc54-g-100579_32	183	0.4	5.3845	1.9	0.0792	0.8	1098	20	1177	15	1177	15
Bc54-g-100579_31	125	0.5	5.3779	2.0	0.0773	0.8	1099	20	1130	16	1130	16
Bc54-g-100579_30	953	0.2	5.8582	2.0	0.0745	0.6	1016	18	1055	12	1055	12
Bc54-g-100579_29	534	0.1	5.7221	1.5	0.0745	0.6	1038	14	1055	12	1055	12
Bc54-g-100579_28	600	0.3	4.6206	1.5	0.0824	0.6	1263	17	1254	11	1254	11

sample name	U	Th/U	238U/206Pb	1 sigma	207Pb/206Pb	1 sigma	206Pb/238U	+/- 1σ	207Pb/206Pb	+/- 1σ	Best age	+/- 1σ
	ppm			% error		% error	age	Ma	age	Ma	Ma	Ma
Bc54-g-100579_27	277	0.6	5.1625	1.5	0.0786	0.6	1141	16	1163	12	1163	12
Bc54-g-100579_26	812	0.1	5.7963	2.0	0.0771	0.6	1026	19	1122	12	1122	12
Bc54-g-100579_24	225	0.7	5.5254	1.8	0.0781	0.7	1072	18	1149	13	1149	13
Bc54-g-100579_23	1992	0.3	5.4837	1.4	0.0737	0.6	1080	14	1034	11	1034	11
Bc54-g-100579_22	247	0.4	4.2022	1.5	0.0924	0.6	1376	19	1476	12	1476	12
Bc54-g-100579_21	1182	0.0	6.0741	1.5	0.0731	0.5	982	13	1017	11	982	13
Bc54-g-100579_20	30	0.9	6.3155	1.8	0.0710	1.3	948	16	958	26	948	16
Bc54-g-100579_19	243	0.4	4.7259	1.5	0.0852	0.6	1237	17	1319	12	1319	12
Bc54-g-100579_17	345	0.6	4.3072	1.4	0.0852	0.6	1346	17	1319	12	1319	12
Bc54-g-100579_15	157	0.4	4.5842	1.5	0.0848	0.7	1272	17	1312	13	1312	13
Bc54-g-100579_14	775	0.5	3.8223	1.5	0.0909	0.5	1498	20	1445	10	1445	10
Bc54-g-100579_13	47	1.6	2.0547	1.5	0.1784	0.7	2556	32	2638	11	2638	11
Bc54-g-100579_12	203	0.4	4.0358	1.5	0.0917	0.6	1427	19	1461	12	1461	12
Bc54-g-100579_11	77	0.4	5.1593	1.5	0.0769	0.8	1142	16	1118	17	1142	16
Bc54-g-100579_10	98	0.1	6.2245	1.5	0.0708	0.9	960	14	953	18	960	14
Bc54-g-100579_9	727	0.2	5.3942	1.5	0.0755	0.6	1096	15	1081	12	1081	12
Bc54-g-100579_6	413	0.4	5.0320	1.5	0.0787	0.6	1168	16	1164	13	1164	13
Bc54-g-100579_5	367	0.2	4.2104	1.6	0.0883	0.6	1374	20	1389	11	1389	11
Bc54-g-100579_3	477	0.3	5.6144	1.4	0.0768	0.6	1057	14	1116	12	1116	12
Bc54-g-100579_2	117	0.9	4.1466	1.9	0.0906	0.8	1393	24	1438	15	1438	15
Bc54-g-100579_1	266	0.5	5.6671	1.4	0.0741	0.6	1048	14	1044	13	1044	13
Bd21-j_3	426	0.2	5.9492	1.9	0.0736	1.0	1002	17	1032	21	1032	21
Bd21-j_4	1590	0.2	6.2960	1.9	0.0732	1.0	950	17	1020	20	1020	20
Bd21-j_5	191	0.3	4.9569	2.0	0.0845	1.2	1185	22	1305	22	1305	22
Bd21-j_7	963	0.4	6.2443	1.7	0.0718	0.9	958	15	980	19	980	19
Bd21-j_8	173	0.3	5.2432	1.7	0.0786	1.1	1125	18	1163	22	1163	22
Bd21-j_9	404	0.3	4.8630	1.7	0.0805	1.0	1206	19	1209	20	1209	20
Bd21-j_10	140	0.7	4.4898	1.6	0.0861	1.1	1296	19	1340	21	1340	21
Bd21-j_11	91	0.4	9.0064	1.8	0.0635	1.5	679	12	725	30	679	12
Bd21-j_15	119	0.3	3.8116	2.0	0.0955	1.1	1502	27	1539	20	1539	20
Bd21-j_16	404	0.4	5.9760	2.1	0.0772	1.0	997	19	1126	20	1126	20

sample name	U	Th/U	238U/206Pb	1 sigma	207Pb/206Pb	1 sigma	206Pb/238U	+/- 1σ	207Pb/206Pb	+/- 1σ	Best age	+/- 1σ
	ppm			% error		% error	age	Ma	age	Ma	Ma	Ma
Bd21-j_17	166	0.7	5.1005	2.0	0.0781	1.1	1154	21	1150	21	1150	21
Bd21-j_19	279	0.3	5.7433	2.1	0.0734	1.1	1035	20	1025	21	1025	21
Bd21-j_20	28	0.9	6.1511	2.4	0.0723	2.2	971	22	995	44	995	44
Bd21-j_23	75	0.6	4.4232	2.0	0.0860	1.3	1314	24	1339	24	1339	24
Bd21-j_25	367	0.8	5.2243	1.9	0.0797	1.0	1129	19	1190	20	1190	20
Bd21-j_30	227	1.3	2.2475	1.8	0.1837	0.9	2373	36	2687	15	2687	15
Bd21-j_33	172	0.3	5.7442	1.8	0.0775	1.1	1035	17	1135	23	1135	23
Bd21-j_34	580	0.3	5.8273	1.7	0.0737	1.0	1021	16	1033	19	1033	19
Bd21-j_39	594	0.0	15.1806	2.1	0.0561	1.4	411	8	455	31	411	8
Bd21-j_40	127	0.2	4.6364	1.7	0.0822	1.1	1259	20	1251	22	1251	22
Bd21-j_41	272	0.3	4.5127	1.6	0.0885	1.0	1290	19	1393	19	1393	19
Bd21-j_44	311	0.4	4.2835	1.6	0.0905	1.0	1353	20	1437	19	1437	19
Bd21-j_45	380	0.2	6.3686	1.7	0.0727	1.0	940	14	1004	20	1004	20
Bd21-j_46	142	0.4	4.0414	1.7	0.0914	0.9	1425	21	1455	17	1455	17
Bd21-j_47	125	0.5	4.2345	1.7	0.0897	1.0	1367	21	1419	19	1419	19
Bd21-j_48	71	0.7	6.9795	1.7	0.0698	1.5	863	13	922	30	922	13
Bd21-j_49	99	0.5	4.5657	1.7	0.0842	1.1	1277	19	1296	22	1296	22
Bd21-j_50	526	0.5	6.1877	1.7	0.0728	1.0	966	15	1007	20	1007	20
Bd21-j_51	612	0.3	6.1914	1.7	0.0723	1.0	965	15	994	20	994	20
Bd21-j_53	305	0.8	8.4887	1.6	0.0640	1.1	718	11	743	23	718	11
Bd21-j_55	194	0.2	8.1432	1.7	0.0666	1.4	747	12	824	29	747	12
Bd21-j_56	208	0.2	5.8728	1.9	0.0769	1.1	1014	18	1118	22	1118	22
Bd21-j_57	615	0.0	14.4160	1.6	0.0560	1.1	432	7	454	24	432	7
Bd21-j_61	1313	0.3	5.0476	1.7	0.0791	0.9	1165	18	1175	18	1175	18
Bd21-j_63	265	0.0	14.2080	2.1	0.0568	1.7	438	9	483	37	438	9
Bd21-j_65	604	0.2	6.0123	1.6	0.0735	0.9	992	15	1028	19	1028	19
Bd21-j_66	220	0.3	6.2701	1.8	0.0747	1.1	954	16	1061	22	1061	22
Bd21-j_67	77	0.3	6.4305	1.7	0.0742	1.5	932	15	1047	30	1047	30
Bd21-j_68	513	0.0	14.7711	1.7	0.0561	1.1	422	7	456	25	422	7
Bd21-j_72	321	0.0	6.1749	1.7	0.0755	1.2	968	16	1082	23	1082	23
Bd21-j_75	71	0.2	5.1527	1.8	0.0795	1.2	1143	19	1184	24	1184	24

sample name	U	Th/U	238U/206Pb	1 sigma	207Pb/206Pb	1 sigma	206Pb/238U	+/- 1σ	207Pb/206Pb	+/- 1σ	Best age	+/- 1σ
	ppm			% error		% error	age	Ma	age	Ma	Ma	Ma
Bd21-j_77	86	0.9	4.3533	1.7	0.0870	1.3	1333	21	1361	25	1361	25
Bd21-j_78	382	0.1	8.4102	1.7	0.0664	1.1	724	12	820	23	724	12
Bd21-j_79	273	0.1	13.6818	3.8	0.0563	3.7	455	17	466	80	455	17
Bd21-j_82	387	0.6	3.9725	1.7	0.0954	1.0	1447	22	1537	18	1537	18
Bd21-j_83	537	0.4	3.4040	1.7	0.1050	0.9	1660	25	1714	17	1714	17
Bd21-j_84	88	0.5	4.3282	1.7	0.0858	1.2	1340	21	1334	22	1334	22
Bd21-j_86	25	0.7	1.9242	1.9	0.1830	1.2	2698	41	2680	20	2680	20
Bd21-j_87	492	0.6	4.0011	1.6	0.0906	0.9	1438	21	1439	17	1439	17
Bd21-j_88	490	0.3	6.0720	1.7	0.0733	1.0	983	16	1022	20	1022	20
Bd21-j_89	152	0.3	8.8299	2.0	0.0634	1.3	692	13	723	27	692	13
Bd21-j_90	549	0.5	3.9121	1.8	0.0936	1.0	1467	24	1500	19	1500	19
Bd21-j_91	232	0.6	4.9915	2.0	0.0798	1.1	1177	22	1191	21	1191	21
Bd21-j_92	363	0.2	6.6679	2.1	0.0729	1.1	901	17	1012	22	1012	22
Bd21-j_93	287	0.6	3.9632	1.9	0.0911	1.1	1450	25	1449	20	1449	20
Bd21-j_95	204	0.7	5.4345	1.7	0.0783	1.0	1089	17	1154	20	1154	20
Bd21-j_96	45	0.6	5.8523	1.9	0.0767	1.7	1017	18	1113	33	1113	33
Bd21-j_97	236	0.6	5.4883	1.7	0.0758	1.1	1079	17	1089	21	1089	21
Bd21-j_100	806	0.3	6.6410	1.7	0.0712	1.0	904	14	964	20	964	20
Bd21-j_102	175	1.1	10.7315	1.9	0.0607	1.4	574	10	629	30	574	10
Bd21-j_104	176	0.4	5.5370	1.9	0.0763	1.2	1070	19	1103	23	1103	23
Bd21-j_105	379	0.3	5.0625	1.8	0.0785	1.0	1162	19	1159	20	1159	20
Bd21-j_107	275	0.1	6.3064	2.3	0.0738	1.0	949	20	1035	21	1035	21
Bd21-j_108	387	0.2	14.2708	2.1	0.0570	1.4	437	9	490	31	437	9
Bd21-j_109	155	0.5	4.1322	1.8	0.0874	1.1	1397	23	1368	21	1368	21
Bd21-j_110	75	0.6	5.0165	1.8	0.0751	1.4	1172	19	1071	29	1071	29
Bd21-j_a_1	122	0.6	9.2956	1.5	0.0611	1.8	659	10	644	37	659	10
Bd21-j_a_2	44	0.7	4.3258	2.1	0.0873	1.5	1341	25	1367	29	1367	29
Bd21-j_a_3	563	0.6	5.6807	1.5	0.0738	1.0	1045	15	1036	20	1036	20
Bd21-j_a_5	104	0.5	4.9603	1.8	0.0770	1.4	1184	20	1121	28	1121	28
Bd21-j_a_8	115	0.3	5.0926	1.7	0.0779	1.3	1156	18	1145	25	1145	25
Bd21-j_a_11	64	0.3	5.0627	1.5	0.0789	1.2	1162	16	1169	24	1169	24

sample name	U	Th/U	238U/206Pb	1 sigma	207Pb/206Pb	1 sigma	206Pb/238U	+/- 1σ	207Pb/206Pb	+/- 1σ	Best age	+/- 1σ
	ppm			% error		% error	age	Ma	age	Ma	Ma	Ma
Bd21-j_a_13	1220	0.3	5.9605	1.3	0.0733	0.9	1000	12	1023	18	1023	18
Bd21-j_a_14	342	0.3	3.6446	1.4	0.1002	1.0	1563	19	1627	18	1627	18
Bd21-j_a_15	96	1.0	5.2856	1.7	0.0830	1.4	1117	17	1269	27	1269	27
Bd21-j_a_16	453	0.3	5.7685	1.8	0.0750	1.0	1031	17	1069	20	1069	20
Bd21-j_a_17	401	0.6	4.5591	1.9	0.0891	1.1	1278	22	1406	20	1406	20
Bd21-j_a_18	102	0.7	3.4401	1.5	0.1005	1.1	1645	22	1633	21	1633	21
Bd21-j_a_19	419	0.3	5.1443	1.4	0.0789	1.0	1145	14	1169	20	1169	20
Bd21-j_a_20	574	0.9	11.5116	1.4	0.0585	1.0	537	7	550	22	537	7
Bd21-j_a_23	129	0.5	5.0246	1.4	0.0786	1.1	1170	15	1163	22	1163	22
Bd21-j_a_26	196	0.8	5.0188	1.4	0.0788	1.1	1171	15	1167	22	1167	22
Bd21-j_a_27	51	0.4	5.4515	1.6	0.0770	1.5	1086	16	1120	29	1120	29
Bd21-j_a_28	442	0.1	4.9812	1.3	0.0799	1.0	1179	14	1195	19	1195	19
Bd21-j_a_29	231	0.3	4.7860	1.3	0.0843	1.1	1223	15	1300	21	1300	21
Bd21-j_a_31	295	0.4	3.9711	1.3	0.0914	0.9	1448	17	1455	18	1455	18
Bd21-j_a_32	995	0.0	14.7396	1.8	0.0549	1.3	423	7	410	29	423	7
Bd21-j_a_33	264	0.4	5.9077	1.4	0.0737	1.0	1008	13	1035	21	1035	21
Bd21-j_a_34	94	0.7	4.2100	1.4	0.0879	1.1	1374	17	1381	22	1381	22
Bd21-j_a_35	933	0.0	5.9899	1.4	0.0726	0.9	995	13	1003	19	1003	19
Bd21-j_a_36	200	0.3	9.1282	1.9	0.0608	1.3	670	12	633	28	670	12
Bd21-j_a_37	179	0.3	4.0544	1.8	0.0904	1.1	1421	23	1433	20	1433	20
Bd21-j_a_38	132	0.6	5.3238	2.1	0.0771	1.2	1110	21	1123	24	1123	24
Bd21-j_a_40	225	0.5	4.9162	1.6	0.0793	1.1	1194	17	1179	21	1179	21
Bd21-j_a_41	411	0.2	4.3197	1.5	0.0862	1.0	1342	19	1343	20	1343	20
Bd21-j_a_42	52	0.8	5.8928	2.1	0.0771	1.7	1010	20	1124	33	1124	33
Bd21-j_a_43	571	0.5	10.6542	1.8	0.0592	1.1	578	10	573	24	578	10
Bd21-j_a_44	234	0.4	4.8644	1.9	0.0833	1.1	1205	21	1276	22	1276	22
Bd21-j_a_46	237	0.3	5.8717	1.7	0.0768	1.2	1014	16	1115	25	1115	25
Bd21-j_a_47	178	0.5	4.6403	2.4	0.0833	1.2	1258	27	1277	23	1277	23
Bd21-j_a_48	182	0.5	5.5058	1.6	0.0732	1.2	1076	16	1019	23	1019	23
Bd21-j_a_50	376	0.2	14.6538	1.5	0.0555	1.4	426	6	434	30	426	6
Bd21-j_a_51	549	0.4	6.0875	1.8	0.0733	1.1	980	16	1022	21	1022	21

sample name	U	Th/U	238U/206Pb	1 sigma	207Pb/206Pb	1 sigma	206Pb/238U	+/- 1σ	207Pb/206Pb	+/- 1σ	Best age	+/- 1σ
	ppm			% error		% error	age	Ma	age	Ma	Ma	Ma
Bd21-j_a_52	110	0.8	4.6805	2.3	0.0850	1.3	1248	27	1314	26	1314	26
Bd21-j_a_53	36	0.8	5.9784	2.8	0.0732	2.1	997	26	1021	42	1021	42
Bd21-j_a_54	151	0.3	4.5136	2.0	0.0842	1.3	1290	23	1297	25	1297	25
Bd21-j_a_56	157	0.3	3.7958	1.7	0.0929	1.1	1507	23	1485	21	1485	21
Bd21-j_a_57	433	0.4	5.0118	1.7	0.0778	1.1	1173	19	1141	21	1141	21
Bd21-j_a_58	125	0.9	6.0058	1.6	0.0719	1.3	993	15	985	26	985	26
Bd21-j_a_59	158	0.3	6.0592	1.8	0.0753	1.3	985	16	1076	26	1076	26
Bd21-j_a_60	553	0.7	5.6473	1.8	0.0740	1.0	1051	17	1041	20	1041	20
Bd21-j_a_61	303	0.3	5.7140	1.9	0.0734	1.2	1040	18	1026	23	1026	23
Bd21-j_a_62	466	0.4	5.2181	1.5	0.0788	1.1	1130	15	1168	21	1168	21
Bd21-j_a_63	131	0.4	4.1199	1.6	0.0914	1.2	1401	20	1454	23	1454	23

Delaware Geological Survey
University of Delaware
Newark, Delaware 19716